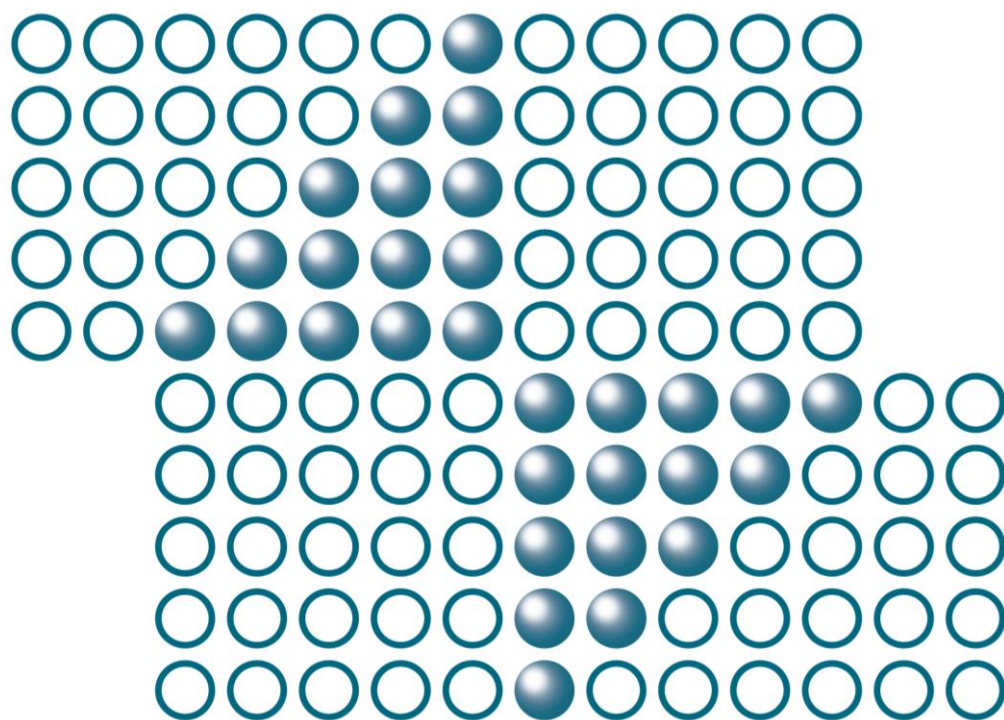


# ABSTRACT BOOKLET

Abstracts of Contributions from the  
18<sup>th</sup> International Symposium on Metallography,  
Fractography and Materials Science

**METALLOGRAPHY & FRACTOGRAPHY 2022**



Edited by

Miloš MATVIJA and Peter HORŇAK

# **ABSTRACT BOOKLET**

Abstracts of Contributions from the  
18<sup>th</sup> International Symposium on Metallography,  
Fractography and Materials Science

**METALLOGRAPHY & FRACTOGRAPHY 2022**

April 27 – 29, 2022

Hotel Atrium\*\*\*  
Nový Smokovec  
High Tatra Mountains  
Slovak Republic

**Edited by**  
Miloš Matvija  
Peter Horňak

**Copyright** © 2022 Technical University of Košice, Slovak Republic

All rights reserved. No part of the contents of this publication may be reproduced or transmitted in any form or by any means without the written permission of the publisher.

Technical University of Košice  
Faculty of Materials, Metallurgy and Recycling  
Institute of Materials and Quality Engineering  
Letná 1/9  
042 00 Košice-Sever  
Slovak Republic

Full text available online at <http://konferencie.net/metal0>

Title / Názov:	Abstract Booklet
Editors / Autori:	Miloš Matvija, Peter Horňak
Publisher / Vydavateľ:	Technical University of Košice / Technická univerzita v Košiciach
Year / Rok:	2022
Edition / Vydanie:	first / prvé
Quantity / Náklad:	80 pcs. / ks
Pages / Rozsah:	68 p. / str.
ISBN:	978-80-553-4064-7

Print / Tlač: EQUILIBRIA, s.r.o., Textilná 4, 040 12 Košice, Slovak Republic

## Organizers

**INSTITUTE OF MATERIALS AND QUALITY ENGINEERING,  
FACULTY OF MATERIALS, METALLURGY AND RECYCLING,  
TECHNICAL UNIVERSITY OF KOŠICE, SLOVAK REPUBLIC**

Letná 1/9, 042 00 Košice-Sever, Slovak Republic

phone: +421 55 602 2543, +421 55 602 2539  
e-mails: peter.hornak@tuke.sk, milos.matvija@tuke.sk  
website: konferencie.net/metalo

**INSTITUTE OF MATERIALS RESEARCH OF THE  
SLOVAK ACADEMY OF SCIENCES  
KOŠICE, SLOVAK REPUBLIC**

Watsonova 47, 040 01 Košice, Slovak Republic

phone: +421 55 792 2402  
e-mail: imrsas@saske.sk  
website: wwwnew.saske.sk/imr/

**LUMAKON, s.r.o.,  
KOŠICE, SLOVAK REPUBLIC**

Na Šajbe 1A, 040 01 Košice, Slovak Republic

phone: +421 903 249 123  
e-mail: metalo@konferencie.net  
website: konferencie.net/metalo

## Co-organizers

**SLOVAK METAL SCIENCE SOCIETY OF THE  
SLOVAK ACADEMY OF SCIENCES, SLOVAK REPUBLIC**

**INSTITUTE OF EXPERIMENTAL PHYSICS OF THE  
SLOVAK ACADEMY OF SCIENCES, KOŠICE, SLOVAK REPUBLIC**

**RESEARCH AND DEVELOPMENT USSE,  
U. S. STEEL KOŠICE, s.r.o., KOŠICE, SLOVAK REPUBLIC**

**ŽP RESEARCH & DEVELOPMENT CENTER s.r.o.,  
PODBREZOVÁ, SLOVAK REPUBLIC**

**Date of the Conference:** April 27 – 29, 2022

**Place of the Conference:** Atrium Hotel, Nový Smokovec,  
High Tatra Mountains, Slovak Republic

## Committees

### CHAIR OF THE SYMPOSIUM

<b>Peter Horňak</b>	Institute of Materials and Quality Engineering, Faculty of Materials, Metallurgy and Recycling, Technical University of Košice, Košice, Slovakia
<b>Pavol Hvizdoš</b>	Institute of Materials Research, Slovak Academy of Sciences, Košice, Slovakia

### INTERNATIONAL SCIENTIFIC COMMITTEE

#### Joint-chairmen

<b>Ján Dusza</b>	Institute of Materials Research, Slovak Academy of Sciences, Košice, Slovakia
<b>Margita Longauerová</b>	Metal Science Society at the Slovak Academy of Sciences, Slovakia
<b>Akio Nishimoto</b>	Kansai University, Osaka, Japan

<b>Katalin Balázs</b>	Hungarian Academy of Sciences, Budapest, Hungary
<b>Pavol Beraxa</b>	ŽP Research & Development Center s.r.o., Podbrezová, Slovakia
<b>Kornel Csach</b>	Institute of Experimental Physics of Slovak Academy of Sciences, Košice, Slovakia
<b>Ľubomír Čaplovič</b>	Faculty of Materials Science and Technology in Trnava, Slovak University of Technology in Bratislava, Trnava, Slovakia
<b>Pavel Diko</b>	Institute of Experimental Physics of Slovak Academy of Sciences, Košice, Slovakia
<b>Jana Dobrovská</b>	Faculty of Materials Science and Technology, VSB - Technical University of Ostrava, Ostrava, Czech Republic
<b>Alistair Doig</b>	Defence Academy of the UK, Shrivenham, United Kingdom
<b>Martin Fújda</b>	Institute of Materials and Quality Engineering, Faculty of Materials, Metallurgy and Recycling, Technical University of Košice, Košice, Slovakia
<b>Roland Haubner</b>	University of Technology Vienna, Institute of Chemical Technologies and Analytics, Vienna, Austria
<b>Peter Horňak</b>	Institute of Materials and Quality Engineering, Faculty of Materials, Metallurgy and Recycling, Technical University of Košice, Košice, Slovakia
<b>Ivan Hrivňák</b>	Slovak University of Technology in Bratislava, Trnava, Slovakia
<b>Christian Chimani</b>	AIT Austrian Institute of Technology GmbH, Wien, Austria
<b>Kenji Ikeuchi</b>	Osaka, Japan
<b>Karol Iždinský</b>	Institute of Materials and Machine Mechanics of Slovak Academy of Sciences, Bratislava, Slovakia
<b>Jozef Janovec</b>	Institute of Materials and Quality Engineering, Faculty of Materials, Metallurgy and Recycling, Technical University of Košice, Košice, Slovakia
<b>Kamila Janovská</b>	Faculty of Materials Science and Technology, VSB - Technical University of Ostrava, Ostrava, Czech Republic
<b>Lucyna Jaworska</b>	AGH Krakow, Poland
<b>Zdeněk Jonšta</b>	Ostrava, Czech Republic
<b>Josef Kasl</b>	Research and Testing Institute Pilsen s.r.o., Pilsen, Czech Republic
<b>Radomila Konečná</b>	Faculty of Mechanical Engineering, University of Žilina, Žilina, Slovakia
<b>Viera Kohuteková</b>	Research and Development USSE, U. S. Steel Košice, s.r.o., Košice, Slovakia
<b>Alexandra Kovalčíková</b>	Institute of Materials Research, Slovak Academy of Sciences, Košice, Slovakia
<b>Ludvík Kunz</b>	Institute of Physics of Materials, Czech Academy of Sciences, Brno, Czech Republic
<b>Pavel Lejček</b>	Institute of Physics, Czech Academy of Sciences, Prague, Czech Republic
<b>Svätoboj Longauer</b>	Metal Science Society at the Slovak Academy of Sciences, Slovakia
<b>Petr Louda</b>	Faculty of Mechanical Engineering, Technical University of Liberec, Liberec, Czech Republic
<b>Maroš Martinkovič</b>	Faculty of Materials Science and Technology in Trnava, Slovak University of Technology in Bratislava, Trnava, Slovakia
<b>Eva Mazancová</b>	Faculty of Materials Science and Technology, VSB - Technical University of Ostrava, Ostrava, Czech Republic
<b>Wojciech Maziarz</b>	Polish Academy of Sciences, Krakow, Poland
<b>Erik Navara</b>	Jihlava, Czech Republic

<b>Peter Palček</b>	Faculty of Mechanical Engineering, University of Žilina, Žilina, Slovakia
<b>Ľudovít Parilák</b>	Košice, Slovakia
<b>Jaroslav Pokluda</b>	Faculty of Mechanical Engineering, Brno University of Technology, Brno, Czech Republic
<b>Karel Saks</b>	Institute of Materials Research, Slovak Academy of Sciences, Košice, Slovakia
<b>František Simančík</b>	Institute of Materials & Machine Mechanics of Slovak Academy of Sciences, Bratislava, Slovakia
<b>Pavol Šajgalík</b>	President, Slovak Academy of Sciences, Bratislava, Slovakia
<b>Jiří Švejcar</b>	Faculty of Mechanical Engineering, Brno University of Technology, Brno, Czech Republic
<b>Elena Tabachnikova</b>	B. Verkin Institute for Low Temperature Physics and Engineering, National Ukraine Academy of Sciences, Kharkov, Ukraine
<b>Eva Tillová</b>	Faculty of Mechanical Engineering, University of Žilina, Žilina, Slovakia
<b>George Vander Voort</b>	Consultant in Metallography, Failure Analysis & Archeometallurgy, USA
<b>Vlastimil Vodárek</b>	Faculty of Materials Science and Technology, VSB - Technical University of Ostrava, Ostrava, Czech Republic
<b>Dalibor Vojtěch</b>	Faculty of Chemical Technology, University of Chemistry and Technology Prague, Prague, Czech Republic
<b>Esa Vuorinen</b>	Luleå University of Technology, Luleå, Sweden
<b>Panyawat Wangyao</b>	Faculty of Engineering, Chulalongkorn University, Bangkok, Thailand
<b>Bogdan Wendler</b>	Technical University of Lodz, Lodz, Poland
<b>Jozef Zrník</b>	Prague, Czech Republic
<b>Petr Zuna</b>	Faculty of Mechanical Engineering, Czech Technical University in Prague, Prague, Czech Republic

#### HONORARY COMMITTEE

<b>Peter Horňák</b>	Chairman of the Symposium, Institute of Materials and Quality Engineering, Faculty of Materials, Metallurgy and Recycling, Technical University of Košice, Košice, Slovakia
<b>Pavol Hvizdoš</b>	Co-Chairman of the Symposium, Director, Institute of Materials Research, Slovak Academy of Sciences, Košice, Slovakia
<b>Ján Dusza</b>	Joint Chairman, Institute of Materials Research, Slovak Academy of Sciences, Košice, Slovakia
<b>Ivan Hrivňák</b>	Founder of the Metallography Symposium
<b>Margita Longauerová</b>	Long Term Chairman of the Metallography Symposium
<b>Pavol Beraxa</b>	Director, ŽP Research & Development Center s.r.o., Podbrezová, Slovakia
<b>James E. Bruno</b>	President of U. S. Steel Košice, s.r.o., Slovakia
<b>Kamila Janovská</b>	Dean, Faculty of Materials Science and Technology, VSB - Technical University of Ostrava, Ostrava, Czech Republic
<b>Martin Fujda</b>	Director, Institute of Materials and Quality Engineering, Faculty of Materials, Metallurgy and Recycling, Technical University of Košice, Košice, Slovakia
<b>Zuzana Gažová</b>	Director, Institute of Experimental Physics of Slovak Academy of Sciences, Košice, Slovakia
<b>Peter Horňák</b>	President, Metal Science Society at the Slovak Academy of Sciences, Slovakia
<b>Stanislav Kmeť</b>	Rector, Technical University of Košice, Košice, Slovakia
<b>Viera Kohuteková</b>	General Manager, Research and Development USSE, U. S. Steel Košice, s.r.o., Košice, Slovakia
<b>Ludvík Kunz</b>	Director, Institute of Physics of Materials, Czech Academy of Sciences, Brno, Czech Republic
<b>Ľudovít Parilák</b>	Founder of ŽP Research & Development Center s.r.o., Podbrezová, Slovakia
<b>Vladimír Soták</b>	President, Železiarne Podbrezová a. s., Slovakia
<b>Pavol Šajgalík</b>	President, Slovak Academy of Sciences, Bratislava, Slovakia
<b>Iveta Vasková</b>	Dean, Faculty of Materials, Metallurgy and Recycling, Technical University of Košice, Košice, Slovakia
<b>Vladimír Zvarík</b>	Member of the Supervisory Board, Železiarne Podbrezová a.s., Podbrezová, Slovakia

**ORGANIZING COMMITTEE**

<b>Peter Horňak</b>	Chairman, Institute of Materials and Quality Engineering, Faculty of Materials, Metallurgy and Recycling, Technical University of Košice, Košice, Slovakia
<b>Pavol Hvizdoš</b>	Co-Chairman, Institute of Materials Research, Slovak Academy of Sciences, Košice, Slovakia
<b>Miloš Matviša</b>	Secretary of the Symposium, Institute of Materials and Quality Engineering, Faculty of Materials, Metallurgy and Recycling, Technical University of Košice, Košice, Slovakia
<b>Tomáš Lukáč</b>	Economic Department of the Symposium, Lumakon, s. r. o., Košice, Slovakia
<b>Martin Fujda</b>	Institute of Materials and Quality Engineering, Faculty of Materials, Metallurgy and Recycling, Technical University of Košice, Košice, Slovakia
<b>Mária Hagarová</b>	Institute of Materials and Quality Engineering, Faculty of Materials, Metallurgy and Recycling, Technical University of Košice, Košice, Slovakia
<b>Viera Horáková</b>	Institute of Materials and Quality Engineering, Faculty of Materials, Metallurgy and Recycling, Technical University of Košice, Košice, Slovakia
<b>Peter Slovenský</b>	Institute of Materials and Quality Engineering, Faculty of Materials, Metallurgy and Recycling, Technical University of Košice, Košice, Slovakia
<b>Beáta Ballóková</b>	Institute of Materials Research of Slovak Academy of Sciences, Košice, Slovakia
<b>Michal Ivor</b>	Institute of Materials Research of Slovak Academy of Sciences, Košice, Slovakia
<b>Erika Múdra</b>	Institute of Materials Research of Slovak Academy of Sciences, Košice, Slovakia
<b>Marek Vojtko</b>	Institute of Materials Research of Slovak Academy of Sciences Košice, Slovakia
<b>Pavel Bekeč</b>	ŽP Research & Development Center s.r.o., ŽP Podbrezová, Slovakia
<b>Mária Demčáková</b>	Research and Development USSE, U. S. Steel Košice, s.r.o., Slovakia
<b>Alica Mašlejová</b>	Research and Development USSE, U. S. Steel Košice, s.r.o., Slovakia
<b>Pavol Zubko</b>	Research and Development USSE, U. S. Steel Košice, s.r.o., Slovakia

## Acknowledgement

The Conference Committee wishes to acknowledge the assistance and encouragement that we have received from several individuals and organizations in the preparation of this event, from companies taking part in the exhibition, and which also sponsor this symposium, are as follows:

### General Advertising Partners:



TESCAN ORSAY HOLDING, a.s.



JEOL Europe SAS



ŽP Research & Development Center s.r.o.

### Advertising Partners:



MATERIÁLOVÝ A METALURGICKÝ VÝZKUM s.r.o.



ZwickRoel s.r.o.



VUJE, a.s



Evonik Fermas s.r.o.



ZENA-R Slovakia, s.r.o.



Magna PT s.r.o.



ANAMET Slovakia s.r.o.

### Exhibitors:



SPECION, s.r.o.



Metalco Testing s.r.o.



Pragolab s.r.o.



Waters Gesellschaft m.b.H., organizační složka



ANAMET Slovakia s.r.o.



JEOL (EUROPE) SAS - organizační složka



Thermo Fisher Scientific

## List of Content

### INVITED LECTURES

#### **Materials for Hydrogen Absorption Storage**

Kušnířová Katarína, Oroszová Lenka, Varcholová Dagmara and SaksI Karel 14

#### **Slag from Modern Copper Production Found in Bergwerk, Burgenland, Austria**

Haubner Roland and Strobl Susanne 15

#### **Metallography and Fractography of High Entropy Ceramics**

Dusza Ján 16

#### **Influence of Surface Machining on Development of Stress Corrosion Cracking of Distribution Wheels of Main Circulation Pump in Nuclear Power Plants**

Dománková Mária, Bárťová Katarína, Magula Vladimír, Brziak Peter, Novák Bronislav, Kicka Tomáš and Jurčo Vladimír 17

### CONFERENCE LECTURES

#### *ADVANCED MATERIALS, NONFERROUS MATERIALS*

#### **Development of Materials for Solid State Hydrogen Storage**

Kušnířová Katarína, Oroszová Lenka, SaksI Karel, Varcholová Dagmara, Lazár Marián, Tóth Lukáš, Jasmínská Natália and Brestovič Tomáš 20

#### **Light-Weight High-Entropy Alloys for Hydrogen Storage**

Varcholová Dagmara, Kušnířová Katarína, Oroszová Lenka and SaksI Karel 21

#### **Comparison of Microstructure and Properties of Monel 400 Nickel-Copper Alloy Prepared by Casting and Laser Powder Bed Fusion Process**

Chlupová Alice, Šulák Ivo, Kuběna Ivo and Kruml Tomáš 22

#### **Development of Biodegradable Zinc-Based Alloys for Biomedical Applications**

Miženková Wanda, Molčanová Zuzana, Ballóková Beáta, SaksI Karel and Zrodowski Lukasz 23

#### **Microstructure Analysis of Progressive Secondary AlSi7Mg0.6 Alloy with Higher Fe Content Using Electron Metallography Techniques**

Pastierovičová Lucia, Kuchariková Lenka, Tillová Eva and Chalupová Mária 24

#### *INTERRELATIONSHIP BETWEEN MICROSTRUCTURE AND MATERIAL PROPERTIES, FATIGUE, BIOMEDICAL MATERIALS*

#### **Characterization of a San Mai Steel Composite for the Manufacture of Knives**

Strobl Susanne and Haubner Roland 25

#### **Microstructure and Fatigue Behavior of High Performance Aluminum Alloy Al2024 Produced by Laser Powder Bed Fusion**

Konečná Radomila, Varmus Tibor, Federico Uriati and Gianni Nicoletto 26

#### **High-Temperature Low Cycle Fatigue of Nickel-Based Superalloy IN738LC**

Šulák Ivo, Chlupová Alice and Obrtlík Karel 27

#### **Investigation of Fatigue Failure in Electric Locomotive Axle**

Pytel Stanislav 28

#### **Analysis of Cracks of Thermostats Casings Made of Brass**

Kašl Josef, Aišman David and Fikřlová Růžena 29

<b>Structure and Properties of FeGaX (X=Tb, Y) Alloys</b> Milyutin Vasily, Bureš Radovan, Fáberová Mária and Birčáková Zuzanna	30
<b>Microstructure-Properties Characterization of Selective Laser Melted Biomedical Co-28Cr-6Mo Alloy</b> Efremenko Bohdan, Zurnadzhy Vadym, Chabak Yuliia, Lekatou Angeliki G., Hornak Peter, Vojtko Marek and Efremenko Vasily	31
<i>PROCESS SIMULATION, METALLOGRAPHIC METHODS, WELDINGS</i>	
<b>Numerical Simulation of the Welding Process During the Main Circulation Pump Impeller Repair</b> Baláž Milan	32
<b>Technology Influence on the Quality of Cladding Layers</b> Viňáš Ján, Brezinová Janette and Brezina Jakub	33
<b>Carbon Fibers Doped by Binary Phosphides as an Electrocatalytic Layer for PEM Electrolysers</b> Bera Cyril and Strečková Magdaléna	34
<b>Application of Copper Powder in Manufacturing of Composite Filament in 3D Printings</b> Dzindziora Agnieszka, Dzienniak Damian and Sułowski Maciej	35
<b>Optimization of Raster Point Deposition Methodology for Deformation Analyses</b> Duchac Alfred and Kejzlar Pavel	36
<b>POSTER PRESENTATION</b>	
<i>METALLOGRAPHIC METHODS</i>	
<b>Automation of Metallographic Sample Etching Process</b> Ambrož Ondřej, Čermák Jan, Jozefovič Patrik and Mikmeková Šárka	38
<b>Identification of Corrosion Mechanisms of Stainless Steel with Metallography Cross Sections</b> Geiplova Hana, Vlachova Marketa and Piskova Anna	39
<b>Highly Accurate Structural Analysis of Austempered Ductile Iron Using EBSD Technique</b> Kejzlar Pavel, Andrsova Zuzana, Petrzilkova Michaela, Skrbek Bretislav and Myszka Dawid	40
<b>A Study of Cut Surface After the Abrasive Water Jet Application on the MS1 Material Prepared by DMLS Method</b> Vandzura Radoslav, Simkulet Vladimir, Botko Frantisek and Gelatko Matus	41
<i>INTERRELATIONSHIP BETWEEN MICROSTRUCTURE AND MATERIAL PROPERTIES</i>	
<b>Analysis of Tribodegradation Factors Limiting the Life of the Molds</b> Brezinová Janette, Miroslav Džupon, Viňáš Ján, Brezina Jakub and Hašul' Ján	42
<b>Stress–Strain State and Texture Evolution in Cold Drawing of Steel Tubes</b> Burik Peter, Bella Peter and Kejzlar Pavel	43
<b>Formation of Sulphides in As-Cast GOES Thin Strips</b> Hradečný Kryštof, Palupčíková Renáta, Volodarskaja Anastasia and Vodárek Vlastimil	44
<b>The Effect of Improper Post Bend Heat Treatment on Microstructure and Properties of a Pipe Bend Made of 0.5Cr-0.5Mo-0.3V Steel</b> Kuboň Zdeněk, Vodárek Vlastimil and Rožnovská Gabriela	45
<b>Correlation of Magnetic Structural and Mechanical Properties of Selected Classes of Microwires</b> Milkovičová Jana, Milkovič Ondrej, Hvizdoš Pavol, Sedlák Richard and Csanádi Tamás	46

<b>Optimization of the Manufacturing Process of Sintered Fe-Mn-Cr-Mo-C Steels Using ANOVA</b> Sułowski Maciej, Matusiewicz Piotr and Kij Piotr	47
<i>FRACTURE</i>	
<b>Dynamic Fracture Characteristics of High-Strength Steel</b> Kianicová Marta, Dlouhý Ivo, Šandera Pavel, Horníková Jana and Pokluda Jaroslav	48
<b>Metallography of Fractured Aluminium Alloys for the Transmission System's Elements</b> Krejslova Katerina and Turek Libor	49
<b>Fracture Mechanisms of Austenitic Steel Caused by Dynamic Tests</b> Uhrčík Milan, Palček Peter, Chalupová Mária, Kuchariková Lenka, Zatkalíková Viera, Belan Juraj, Oravcová Monika and Pastierovičová Lucia	50
<i>FATIGUE</i>	
<b>The Fractographic Analysis of Static and Fatigue Fracture Surfaces in Secondary A356 Aluminum Alloy With a Higher Concentration of Iron</b> Kuchariková Lenka, Tillová Eva, Chalupová Mária, Uhrčík Milan, Pastierovičová Lucia and Belan Juraj	51
<i>ADVANCED MATERIALS</i>	
<b>Microstructure Characterization of Fe-Based Nanomaterials by High-Energy X-ray Scattering Techniques</b> Baldovský Andrej, Yudina Daria, Girman Vladimír, Lisnichuk Maksym, Sovák Pavol and Bednarčík Jozef	52
<b>Thermal Shock Resistance of Ultra High Temperature ZrB<sub>2</sub> Ceramic Composites</b> Ivor Michal, Kovalčíková Alexandra and Dusza Ján	53
<b>Ceramic Nano/Microfibers as Filler for Composites</b> Koribanich Ihor, Mudra Erika, Kovalcikova Alexandra, Shepa Ivan, Girman Vladimir, Hrubovcakova Monika, Pavlinak David, Balaz Matej and Dusza Jan	54
<b>Microstructural Analysis of EuBCO Bulks With and Without Holes</b> Kuchárová Veronika, Diko Pavel, Lojka Michal, Hlásek Tomáš and Plecháček Vladimír	55
<b>Influence of Ligands on Physicochemical Characteristics of Magnetic Nanoparticles</b> Szucsova Jaroslava, Zelenakova Adriana, Nagy Lubos, Barutiak Michael, Benova Eva, Zelenak Vladimir and Zavisova Vlasta	56
<b>Processing and Mechanical Properties of (Hf-Ta-Zr-Nb-Ti)C</b> Timkova Lenka, Csanadi Tamas, Hrubovcakova Monika, Kovalcikova Alexandra, Naughton Duszova Annamaria, Vaskova Iveta and Dusza Jan	57
<b>Microstructure of YBCO Bulk Samples Grown via 45°-Twin-Seeds</b> Zmorayova Katarina, Diko Pavel and Yao Xin	58
<i>NONFERROUS MATERIALS</i>	
<b>Development and Research of Copper Filter for Full Face Masks Prepared by Powder Metallurgy Technology</b> Ballóková Beáta, Molčanová Zuzana, Brestovič Tomáš, Jasminská Natália, Michalik Štefan and SaksI Karel	59
<b>Formation of Alpha-Case Layer During Oxidation of Ti6Al4V Surface by Annealing at 1050 °C and Change of Microstructure After Different Cooling Rates</b> Belan Juraj, Uhrčík Milan, Kucháriková Lenka, Tillová Eva and Pastierovičová Lucia	60
<b>Direct Production of Tin Bronzes from Copper and Cassiterite</b> Haubner Roland and Strobl Susanne	61

- Influence of Cavitation in Seawater on the Etching Attack of Manganese-Aluminum-Bronzes (MAB)**  
Linhardt Paul, Biezma Maria Victoria, Strobl Susanne and Haubner Roland 62

*BIOMEDICAL MATERIALS*

- The Yttrium Substitution Impact on the Mechanical Properties of Biodegradable Mg<sub>66</sub>Zn<sub>30</sub>Ca<sub>4</sub> Alloy**  
Molčanová Zuzana, Ballóková Beáta, Miženková Wanda, Džupon Miroslav, Zalka Dóra  
and SaksI Karel 63

*DIGITAL IMAGE PROCESSING METHODS*

- Evaluation of Sample Preparation Importance for Digital Image Correlation During Cold Deformation**  
Brlić Tin, Jandrlíć Ivan and Mrkobrada Lorena 64

*WELDING*

- Creep Resistance and Microstructure Evolution in HR3C–P92 Heterogeneous Welds**  
Vodárek Vlastimil, Kuboň Zdeněk, Váňová Petra, Palupčíková Renáta and Langer Svatopluk 65

**EXHIBITOR PRESENTATION**

- From Data to Information with Selective BSE Contrast Methods of TESCAN's CLARA Field-Free UHR-SEM**  
Moravčík Igor 68



# **INVITED LECTURES**

## Materials for Hydrogen Absorption Storage

Kušnířová Katarína<sup>1,a</sup>, Oroszová Lenka<sup>1,b</sup>, Varcholová Dagmara<sup>1,2,c</sup>  
and Saksl Karel<sup>1,2,3,d\*</sup>

<sup>1</sup>Institute of Materials Research, SAS, Watsonova 47, 040 01 Košice, Slovakia

<sup>2</sup>Faculty of Materials, Metallurgy and Recycling, TUKE, Letná 9, 042 00 Košice, Slovakia

<sup>3</sup>Faculty of Science, UPJŠ, Šrobárova 2, 041 54 Košice, Slovakia

<sup>a</sup>kkusnirova@saske.sk, <sup>b</sup>loroszova@saske.sk, <sup>c</sup>dvarcholova@saske.sk, <sup>d\*</sup>ksaksl@saske.sk

**Keywords:** hydrogen; hydrogen storage; metal hydride; high-entropy alloys.

### Abstract.

The declining cost of electricity from renewable sources is providing a path towards a future sustainable, green and carbon neutral energy systems. In terms of operation, their main disadvantage however is intermittency in the process of electricity supply. In this context, batteries have gained interest as a potential energy storage solution, but the amount of possible stored energy is rather limited by current battery chemistries. For comparison, today's most advanced batteries have an energy density per unit weight of 0.5kWh/kg, while hydrogen (H<sub>2</sub>) as another type of energy carrier has an energy density approximately 66x higher 33.3kWh/kg (142 MJ/kg), what from the first impression, clearly prefers hydrogen as an energy carrier. In hydrogen storage technology H/H<sub>2</sub> compression is considered to be the main challenge.

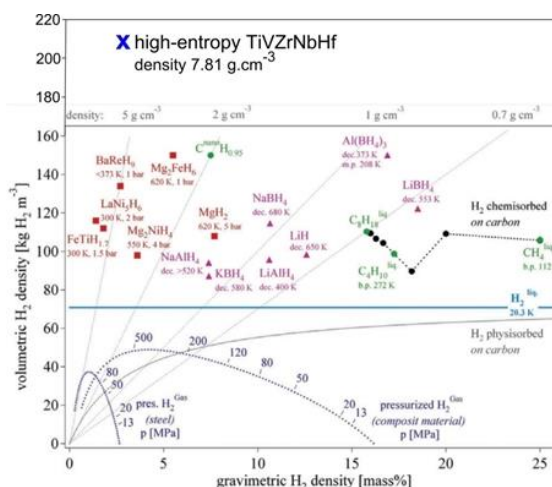


Fig. 1 Volume and gravimetric density of hydrogen of some selected hydrides.  
The picture was taken from [1] and supplemented by K. Saksl.

Fig. 1 shows that the most efficient hydrogen compression method is absorption in a crystal lattice followed by formation of metal hydrides. Among them, today the most promising material are high-entropy alloys capable to store up to 219 kg H<sub>2</sub> in one m<sup>3</sup>, corresponding to the capacity 8.5 kWh/l, value close to the energy density of gasoline 9.5 kWh/l. Team at the IMR SAS headed by Dr. K. Saksl is the only in Slovakia developing such new metallic alloys for hydrogen storage.

### Acknowledgment

The abstract was prepared by the support of the projects: APVV-20-0205 and VEGA 2/0039/22.

### References

[1] Züttel, A., Materials for hydrogen storage, *Mater. Today* 6 (2003) 24–33.

## Slag from Modern Copper Production Found in Bergwerk, Burgenland, Austria

Haubner Roland<sup>1,a\*</sup> and Strobl Susanne<sup>1,b</sup>

<sup>1</sup>Technische Universität Wien, Institute of Chemical Technologies and Analytics, Getreidemarkt 9/164-03, A-1060 Vienna, Austria

<sup>a\*</sup>roland.haubner@tuwien.ac.at, <sup>b</sup>susanne.strobl@tuwien.ac.at

**Keywords:** copper slag; microstructure; archaeometallurgy.

### Abstract.

Bergwerk is a small village in the district of Oberwart in Burgenland. Its Hungarian name was Öribanya. In the 17<sup>th</sup> century copper and iron were mined and smelted. During an archaeological excavation in 1985 K. Kaus collected the examined slags.

These slags are typical plate slags but metallographic studies have shown that these slags are atypical compared to alpine slags (Fig. 1a) [1]. There is an elongated texture running across the slag but the typical fayalite dendrites are absent (Fig. 1b). Relatively high S contents were measured by SEM-EDX and XRF, in addition to the already present O, indicating that both FeO and FeS are present in the slag (Fig. 1b, c, d). The glass phase containing all the slag impurities is located between the fayalite and the FeO-FeS mixture.

Due to the high S content in the slag, there are deviations in percentages of the calculations for the FeO-SiO<sub>2</sub>-CaO phase diagram. However, the measured and calculated values are predominantly in the FeO-rich phase areas.

It has not yet been clarified whether this method of copper extraction has technological advantages.

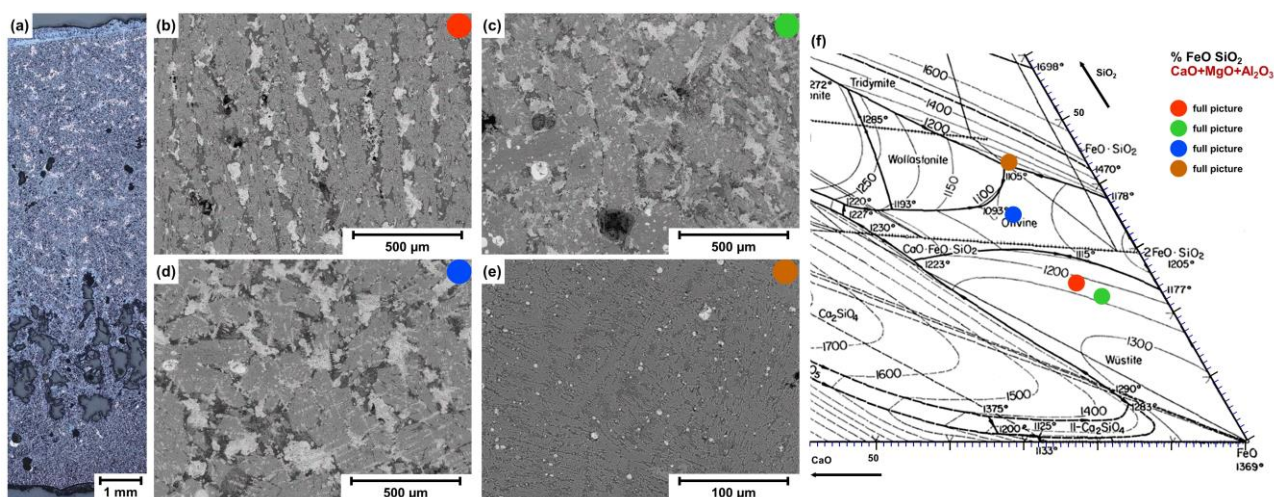


Fig. 1 Copper slag samples from Bergwerk. (a) cross section in LOM, (b – e) different slag microstructures in SEM, (f) EDX measurements of the microstructures shown in Fig. 1b – e, were calculated to plot them in the phase diagram.

### References

- [1] R. Haubner, S. Strobl, S. Klemm, Investigations of a slag from copper smelting discovered at the Bronze Age site Prein VII/Cu in Lower Austria, *Archaeometallurgy in Europe IV. Bibliotheca Praehistorica Hispana*, Vol. 33. Editorial CSIC, Madrid. (2017) 135-142.

## Metallography and Fractography of High Entropy Ceramics

Dusza Ján

Institute of Materials Research, Slovak Academy of Sciences,  
Watsonova 47, 040 01 Košice, Slovakia

[jdusza@imr.saske.sk](mailto:jdusza@imr.saske.sk)

**Keywords:** microstructure; fracture; high entropy ceramics; nano/micro testing.

### Abstract.

The microstructure and fracture characteristics of different high entropy ceramics – carbides, nitrides, carbonitrides, dual – phase systems, etc, were investigated connected with the processing routes and nano/micro mechanical testing of these systems. The microstructure and fracture characteristics were investigated using X-ray diffraction (XRD), scanning electron microscopy (SEM) in combination with electron back scattered diffraction (EBSD) and transmission electron microscopy (TEM). Atomic structure and local chemical disorder were determined by means of scanning transmission electron microscopy (STEM) in conjunction with energy dispersive X-ray spectroscopy (EDS)

Depth-sensing nano-indentation of differently oriented grains and bulk systems has been applied to study the nano/micro hardness and deformation characteristics. Micro-compression tests of micropillars prepared by focused ion beam from oriented facets of grains were studied. During micro-cantilever tests in bending deformation and fracture characteristics of individual grains and grain boundaries have been investigated. The hardness values of differently orientated grains showed significant angle dependence. A strong influence of the grains orientation on compressive yield stress and rupture stress values was found during the micropillar test, too. The active slip systems for individual systems have been recognized. The bending strength of micro-cantilevers was strongly dependent on the character/size of the present fracture origins which were in all cases in nano-metric range. The fracture toughness of the individual grains and grain boundaries were investigated, too.

## Influence of Surface Machining on Development of Stress Corrosion Cracking of Distribution Wheels of Main Circulation Pump in Nuclear Power Plants

Dománková Mária<sup>1,a\*</sup>, Bártová Katarína<sup>1,b</sup>, Magula Vladimír<sup>2,c</sup>, Brziak Peter<sup>2,d</sup>,  
Novák Bronislav<sup>2,e</sup>, Kicka Tomáš<sup>3,f</sup> and Jurčo Vladimír<sup>3,g</sup>

<sup>1</sup>Slovak University of Technology in Bratislava, Faculty of Materials Science and Technology in Trnava, Ulica Jána Bottu 25, Slovakia

<sup>2</sup>Welding Research Institute, Račianska 71, Bratislava, Slovakia

<sup>3</sup>Science and Research Centre Ltd, Kalná nad Hronom, Mochovce 6, Slovakia

<sup>a\*</sup>maria.domankova@stuba, <sup>b</sup>katarina.bartova@stuba.sk, <sup>c</sup>magulav@vuz.sk, <sup>d</sup>brziakp@vuz.sk,  
<sup>e</sup>novakb@vuz.sk, <sup>f</sup>tomas.kicka@cvv.sk, <sup>g</sup>vladimir.jurco@cvv.sk

**Keywords:** microstructure; austenitic stainless steel; stress corrosion cracking.

### Abstract.

Austenitic stainless steels belong to important construction materials due to their suitable combination of mechanical, technological and physical properties. However, their properties, such as e.g., corrosion resistance can be very significantly degraded by improper state of the microstructure. As some experience from technical practice and subsequent studies show, corrosion cracking can also be initiated by the condition of the steel surface.

The surface of the analysed distribution wheel was damaged by a dense network of fine cracks without preferential orientation (Fig.1a). The network of cracks was interrupted by coarse axial cracks, more or less regularly distributed around the circumference of the distribution wheel. Fine and shallow cracks on the surface apparently initiated and grew due to corrosion damage (Fig.1b). An increased occurrence of deformation twins (Fig.1b) and deformation-induced martensite was found in the surface layer of the distribution wheel. The microhardness of the surface layer was increased approximately twofold compared to the microhardness of the matrix, but locally reached up to 400 HV 0.01 (Fig.1c).

The conditions for corrosion cracking were mostly due to specific conditions on the wheel surface and especially to the shortcomings of the surface machining, which caused disproportionately increased hardness and high levels of residual stresses near the wheel surface.

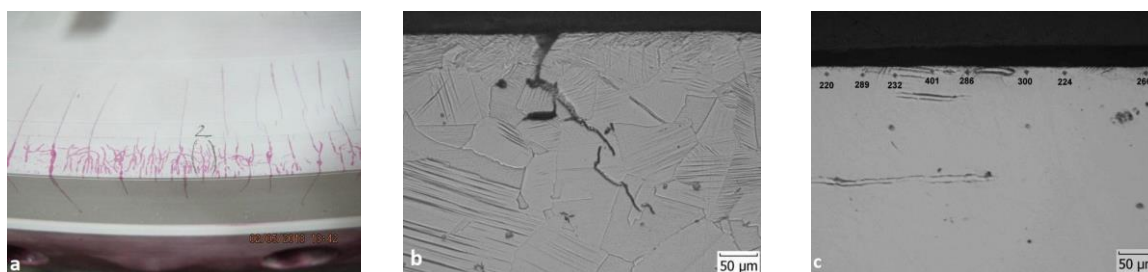


Fig.1 a) Cracks on the distribution wheel surface, b) cross section of the crack network area, c) measured microhardness values HV 0.01 near the surface.

### Acknowledgment

"This research is the result of support under the Operational Program Integrated Infrastructure for the project: Research of corrosion and corrosion cracking in the pressure systems of the primary circuit of nuclear power plants, NFP313020W996, co-financed by the European Regional Development Fund."



# **CONFERENCE LECTURES**

## Development of Materials for Solid State Hydrogen Storage

Kušnírová Katarína<sup>1,a\*</sup>, Oroszová Lenka<sup>1,b</sup>, Saksli Karel<sup>1,2,3,c</sup>,  
Varcholová Dagmara<sup>1,2,d</sup>, Lazár Marián<sup>4,e</sup>, Tóth Lukáš<sup>4,f</sup>, Jasminská Natália<sup>4,g</sup>  
and Brestovič Tomáš<sup>4,h</sup>

<sup>1</sup>Institute of Materials Research, Slovak Academy of Sciences,  
Watsonova 47, 040 01 Košice, Slovak Republic

<sup>2</sup>Faculty of Materials Metallurgy and Recycling, Technical University of Košice,  
Letná 9, 042 00 Košice, Slovak Republic

<sup>3</sup>Faculty of Science, Institute of Physics, Pavol Jozef Šafárik University in Košice,  
041 80 Košice, Slovak Republic

<sup>4</sup>Faculty of Mechanical Engineering, Technical University of Košice,  
Letná 9, 042 00 Košice, Slovak Republic

<sup>a\*</sup>kkusnirova@saske.sk, <sup>b</sup>loroszova@saske.sk, <sup>c</sup>ksaksl@saske.sk, <sup>d</sup>dvarcholova@saske.sk,  
<sup>e</sup>marian.lazar@tuke.sk, <sup>f</sup>lukas.toth@tuke.sk, <sup>g</sup>natalia.jasminska@tuke.sk,  
<sup>h</sup>tomas.brestovic@tuke.sk

**Keywords:** Hume-Rothery rules; high entropy alloys; solid state hydrogen storage; solid solution.

### Abstract.

Series of high entropy alloys designed on Hume-Rothery rules were prepared and the probability of the empirical approach to hydrogen storage materials preparation was investigated. Calculated HEA's with equimolar compositions were selected from the list of alloys with limited VEC (valence electron concentration),  $\Delta S$  and  $\Delta H$ . The phase composition of prepared materials was compared with the prediction model and material characteristics such as chemical composition, density and microhardness were studied. In Table 1 the list of predicted materials is shown together with the calculated characteristics. Related to the thermodynamic properties of calculated alloys valence electron concentration might affect the storage properties of single-phase HEA and maximum concentration of  $H/M = 2$  in alloys with  $VEC < 4.74$  [1].

In this article material characterization of predicted HEA with various VEC values will be presented in terms of empirical prediction methods for solid-state hydrogen storage materials.

Table 1 List of HEA based on prediction model together with the characteristics of VEC,  $\Delta S$ ,  $\Delta H$ ,  $\Omega$  and  $\Delta R$

composition	$\Delta H$	$\Delta S$	$\Omega$	VEC	$\Delta R$
TiVCrCuNb	-0.96	13.38	28.78	6.2	6.24
TiZrNbMoHf	-1.6	13.38	20.26	4.6	6.10
VNbMoHfTa	-1.92	13.38	18.80	5	6.22

### Acknowledgment

The abstract was prepared by the support of the projects: APVV-20-0205, VEGA 2/0039/22 and EIGJAPAN\_JC2021-045.

### References

- [1] M.M. Nygård, G. Ek, D. Karlsson, M.H. Sørby, M. Sahlberg, B.C. Hauback, Counting electrons - a new approach to tailor the hydrogen sorption properties of high- entropy alloys, *Acta Mater.* 175 (2019) 121–129, <https://doi.org/10.1016/j.actamat.2019.06.002>.

## Light-Weight High-Entropy Alloys for Hydrogen Storage

Varcholová Dagmara<sup>1,2,a\*</sup>, Kušnírová Katarína<sup>1</sup>, Oroszová Lenka<sup>1</sup>  
and SaksI Karel<sup>1,2,3</sup>

<sup>1</sup> Institute of Materials Research, Watsonova 47, 040 01 Košice, Slovakia

<sup>2</sup> Faculty of Materials, Metallurgy and Recycling, TUKE, Letná 9, 042 00 Košice, Slovakia

<sup>3</sup> Faculty of Science, UPJŠ Šrobárova 2, 041 54 Košice, Slovakia

<sup>a\*</sup>e-mail of the corresponding author: dvarcholova@saske.sk

**Keywords:** hydrogen; hydrogen storage; metal hydride; high-entropy alloys.

### Abstract.

Hydrogen, as an energy carrier, is gaining prominence due to its exceptional properties. The purity and inexhaustibility of its resources are the basic preconditions for successful application in a wide range of industries. In June 2020, the European Commission identified the Union's flagship technologies, stating that hydrogen and the hydrogen economy were among the key technologies for the future of industry in the European Union. High- entropy alloys have the highest volume hydrogen storage of all materials used so far. In a recent study by Sahlberg et. Al. proved that the highly entropic alloy TiVZrNbHf is to store a large amount of hydrogen up to 210 kg.m<sup>-3</sup>, which is 2.5 to the ratio of hydrogen to metal atoms (H / M). [1] The alloys we create will consist of several elements with low specific gravities. Al<sub>2</sub>Ti<sub>2</sub>Nb<sub>2</sub>X<sub>2</sub>, X = Zr, Hf, V with different atomic fraction. Samples, which were prepared by arc melting and grinding, were subjected to chemical, structural, macroscopic and storage experiments. All the samples prepared by us were subjected to gravimetric high-pressure analysis of hydrogen absorption and desorption.

Table 1 Result table with sorption analysis

Alloy	Alternative alloy	Absorption H [wt. %], [H/M]	Residual H [wt. %],[H/M]	Desorption H [wt.%],[H/M]
Al <sub>30</sub> Ti <sub>30</sub> Nb <sub>15</sub> Zr <sub>25</sub>	Al <sub>30</sub> Ti <sub>35</sub> Nb <sub>15</sub> Zr <sub>20</sub>	1.28/0.74	0.46/0.26	0.82/0.48
Al <sub>20</sub> Ti <sub>20</sub> Nb <sub>35</sub> Zr <sub>25</sub>	Al <sub>23</sub> Ti <sub>25</sub> Nb <sub>30</sub> Zr <sub>22</sub>	1.06/0.69	0.25/0.16	0.81/0.53
Al <sub>30</sub> Ti <sub>30</sub> Nb <sub>25</sub> Zr <sub>15</sub>	Al <sub>30</sub> Ti <sub>35</sub> Nb <sub>20</sub> Zr <sub>15</sub>	0.98/0.54	0.27/0.15	0.71/0.39
Al <sub>20</sub> Ti <sub>20</sub> Nb <sub>25</sub> Zr <sub>35</sub>	Al <sub>25</sub> Ti <sub>25</sub> Nb <sub>20</sub> Zr <sub>30</sub>	1.23/0.82	0.41/0.27	0.82/0.55
<b>Al<sub>15</sub>Ti<sub>35</sub>Nb<sub>25</sub>Zr<sub>25</sub></b>	<b>Al<sub>15</sub>Ti<sub>38</sub>Nb<sub>23</sub>Zr<sub>24</sub></b>	<b>1.61/1.05</b>	<b>0.62/0.40</b>	<b>0.99/0.65</b>
Al <sub>35</sub> Ti <sub>15</sub> Nb <sub>25</sub> Zr <sub>25</sub>	Al <sub>35</sub> Ti <sub>20</sub> Nb <sub>25</sub> Zr <sub>20</sub>	0.79/0.48	0.18/0.10	0.61/0.38
Al <sub>30</sub> Ti <sub>30</sub> Nb <sub>20</sub> Zr <sub>20</sub>	Al <sub>30</sub> Ti <sub>40</sub> Nb <sub>15</sub> Zr <sub>15</sub>	1.10/0.63	0.37/0.22	0.73/0.41
Al <sub>20</sub> Ti <sub>20</sub> Nb <sub>30</sub> Zr <sub>30</sub>	Al <sub>20</sub> Ti <sub>25</sub> Nb <sub>25</sub> Zr <sub>30</sub>	1.28/0.86	0.43/0.29	0.85/0.57
Al <sub>15</sub> Ti <sub>35</sub> Nb <sub>15</sub> Zr <sub>35</sub>	Al <sub>20</sub> Ti <sub>40</sub> Nb <sub>15</sub> Zr <sub>25</sub>	1.28/0.79	0.54/0.33	0.74/0.46
Al <sub>15</sub> Ti <sub>35</sub> Nb <sub>35</sub> Zr <sub>15</sub>	Al <sub>15</sub> Ti <sub>40</sub> Nb <sub>30</sub> Zr <sub>15</sub>	1.33/0.88	0.30/0.20	1.03/0.68

Tab. 1 shows results of sorption analysis measured by gravimetric high-pressure analysis of absorption and desorption at higher temperatures. Sample Al<sub>15</sub>Ti<sub>35</sub>Nb<sub>25</sub>Zr<sub>25</sub> reach values of absorption like commercial alloy.

### Acknowledgment

The abstract was prepared by the support of the projects: APVV-20-0205 and VEGA 2/0039/22.

### References

[1] Züttel, A., Materials for hydrogen storage, *Mater. Today* 6 (2003) 24–33.

## Comparison of Microstructure and Properties of Monel 400 Nickel-Copper Alloy Prepared by Casting and Laser Powder Bed Fusion Process

Chlupová Alice<sup>1,a\*</sup>, Šulák Ivo<sup>1,b</sup>, Kuběna Ivo<sup>1,c</sup> and Kruml Tomáš<sup>1,d</sup>

<sup>1</sup>Institute of Physics of Materials, Academy of Sciences of the Czech Republic, Žižkova 22, 616 00 Brno, Czech Republic

<sup>a\*</sup>chlupova@ipm.cz, <sup>b</sup>sulak@ipm.cz, <sup>c</sup>kubena@ipm.cz, <sup>d</sup>kruml@ipm.cz

**Keywords:** Monel 400; microstructure; properties; fractography; casting; laser powder bed fusion.

### Abstract.

Monel 400 nickel-copper alloy is commonly used in highly corrosive conditions where strength is required. Typical applications are in the marine sector, petrochemical industry or energy facilities as chemical tubes, pumps, heat exchangers and superheated steam systems. This paper compares the microstructure and properties of a cast alloy and the same material prepared by a laser powder bed fusion (LPBF) process. Small cylindrical specimens were used for tensile tests at room temperature and elevated temperatures up to 750 °C in air. The tensile stress-strain response was determined for both types of materials (see Fig. 1a). An increase in test temperature is associated with a decrease in strength. In RT, LPBF material has a higher yield strength and ultimate tensile strength than a cast alloy. At elevated temperatures, the strength of both variants is comparable. However, the fracture elongation of the LPBF material is significantly lower over the entire test temperature range. Fracture surfaces (see Fig. 1b) and polished sections parallel to the sample axis were investigated to compare the typical microstructure (see Fig. 1c) and damage mechanisms of LPBF material variant with an alloy prepared by conventional casting.

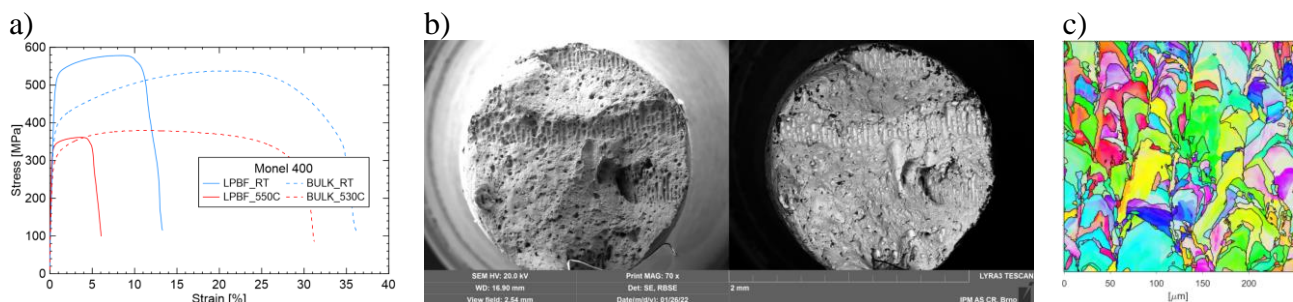


Fig. 1 Comparison of tensile properties at RT and elevated temperature of cast and LPBF variants (a) of Monel 400. SEM micrograph of fracture surface after tensile test of LPBF sample at RT (b) and EBSD map of LPBF microstructure (c).

### Acknowledgment

The present work was conducted in the frame of project funded from the European Union's Horizon 2020 research and innovation programme under grant agreement No 958192.

## Development of Biodegradable Zinc-Based Alloys for Biomedical Applications

Miženková Wanda<sup>1,2,a\*</sup>, Molčanová Zuzana<sup>1</sup>, Ballóková Beáta<sup>1</sup>, Saksí Karel<sup>1</sup> and Zrodowski Lukasz<sup>3</sup>

<sup>1</sup>Institute of Materials Research, SAS, Watsonova 47, 040 01 Košice, Slovakia

<sup>2</sup>Technical University of Kosice, Faculty of Mechanical Engineering, Department of Biomedical Engineering and Measurement

<sup>3</sup>MAZEMET Sp.zo.o., Al.Jana Pawla II 27, Warsaw, Poland

<sup>a\*</sup>wmizenkova@saske.sk

**Keywords:** biodegradable materials; zinc – based alloys; 3D printing.

### Abstract.

Biodegradable biomaterials (BM) consist of elements that occur in human body. BM subsequently degrade in human body after fulfilling their mission in tissue healing process. The product of the degradation are not toxic and are fully resorbable. In this paper we present results of production biodegradable Zinc-based alloys by gravity casting and their processing to obtain better mechanical properties. Dominant element in these types of alloys is Zinc. We develop completely new ternary alloys Zn-0,4Mg-0,4Ca-xMn (x=0, 0,2, 0,4, 0,6, 0,8, 1,1 wt%) - elements Mg, Ca, Mn, stabilize the solid solution and increase the toughness and strength of the alloy. EDX analysis, XRD analysis were performed to show real chemical composition and lattice parameters of prepared alloys. Pre-alloys were processed by overpressure casting of the melt into the Cu mold which allows refinement of the grain. Measurements of microhardness HV<sub>0,1</sub> on pre-alloys and after rapid colling were performed. The metal powder of these type of alloys was prepared by Poland company AMAZEMET. Metal powder will be used in additive manufacturing in the production of the intracorponeal body implants.

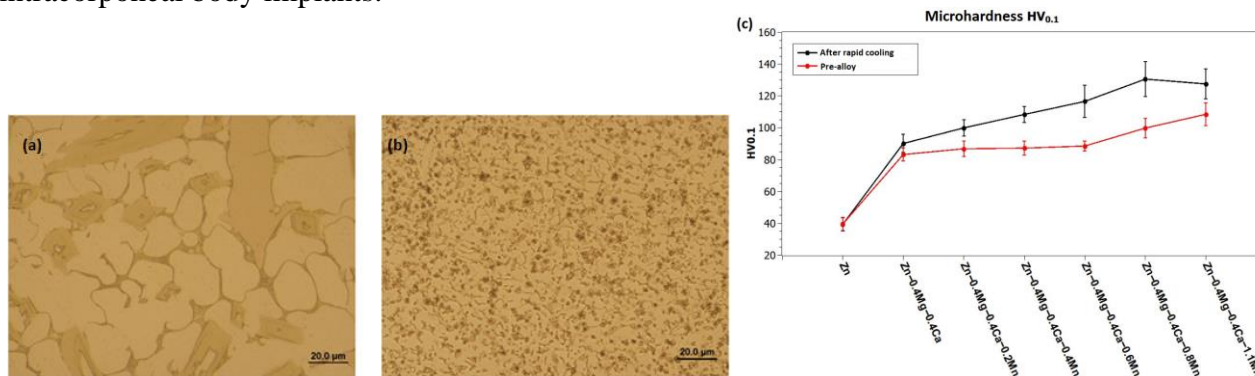


Fig. 1 Typical optical micrographs and microhardness of Zn-0,4Mg-0,4Ca-xMn: (a) Zn-0,4Mg-0,4Ca-1,1Mn cast, (b) Zn-0,4Mg-0,4Ca-1,1Mn after rapid cooling, (c) changes in hardness of Zn-0,4Mg-0,4Ca-xMn with respect to Mn concentrations.

Fig. 1 shows that rapid cooling affects the microstructure. Grain refinement increases the hardness as well as the addition of manganese. The highest microhardness value of  $130.6 \pm 6.0$  was measured for the Zn-0.4Mg-0.4Ca-0.8Mn alloy after rapid cooling. With the addition of Mn, the hardness increased on average by 30% for pre-alloys, by 40% for rapid cooling alloys. The hardness was increased by an average of 25% by rapid cooling process.

### Acknowledgment

The abstract was prepared by the support of the projects: APVV-20-0068.

## Microstructure Analysis of Progressive Secondary AlSi7Mg0.6 Alloy with Higher Fe Content Using Electron Metallography Techniques

Pastierovičová Lucia<sup>1,a\*</sup>, Kuchariková Lenka<sup>1,b</sup>, Tillová Eva<sup>1,c</sup>  
and Chalupová Mária<sup>1,d</sup>

<sup>1</sup>University of Žilina, Faculty of Mechanical Engineering, Department of Materials Engineering, Univerzitná 8215/1, 010 26 Žilina, Slovak Republic

<sup>a\*</sup>lucia.pastierovicova@fstroj.uniza.sk, <sup>b</sup>lenka.kucharikova@fstroj.uniza.sk,  
<sup>c</sup>eva.tillova@fstroj.uniza.sk, <sup>d</sup>maria.chalupova@fstroj.uniza.sk

**Keywords:** secondary alloys; heat treatment; Fe intermetallic phases; deep etching; higher Fe content.

### Abstract.

This article investigates the effect of the higher iron content on the formation of brittle iron-rich needles phases in secondary AlSi7Mg0.6 alloy. These secondary-recycled alloys contain an increased amount of impurities. The common impurity found in these alloys is iron. Higher Fe content negatively affects the structure and mechanical properties. Removing iron from the alloy is a difficult process, so its content is reduced to an acceptable limit. Heat treatment can eliminate negative effect of Fe, whereby influences the size and morphology of structural components. In this study, the T6 heat treatment was applied on the secondary AlSi7Mg0.6 alloy. The chemical composition of AlSi7Mg0.6 according to the delivery list is shown in Table 1. Changes influenced by heat treatment and higher Fe content are evaluated using a scanning electron microscope, including methods of EDX analysis, and methods of deep etching (Fig. 1).

Table 1 Chemical composition of experimental alloys [wt. %]

AlSi7Mg0.6	Si	Fe	Cu	Mn	Mg	Zn	Ti	V	Al
Melt A	6.440	<b>0.155</b>	0.015	0.048	0.625	0.014	0.108	0.015	remainder
Melt B	6.840	<b>0.266</b>	0.012	0.053	0.462	0.016	0.096	0.011	remainder
Melt C	6.340	<b>0.352</b>	0.009	0.041	0.460	0.012	0.102	0.014	remainder

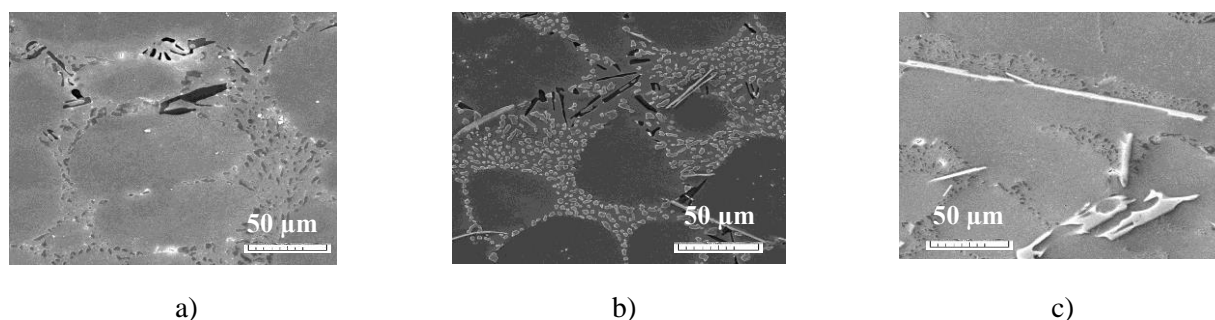


Fig. 1 The microstructure of AlSi7Mg0.6 alloys, etch. 0.5 % HF, SEM.

a) melt A – 0.155 % wt. Fe; b) melt B – 0.226 % wt. Fe; c) melt C – 0.352 % wt. Fe, etch. 0.5% HF, SEM.

### Acknowledgment

The research was supported by Scientific Grand Agency of Ministry of Education of Slovak Republic and Slovak Academy of Sciences, VEGA 01/0398/19, KEGA 016ŽU-4/2020 and project to support young researchers at UNIZA, ID of project 12715—project leader Ing. Lenka Kuchariková Ph.D.

## Characterization of a San Mai Steel Composite for the Manufacture of Knives

Strobl Susanne<sup>1,a</sup> and Haubner Roland<sup>1,b\*</sup>

<sup>1</sup>Technische Universität Wien, Institute of Chemical Technologies and Analytics, Getreidemarkt 9/164-03, A-1060 Vienna, Austria

<sup>a</sup>susanne.strobl@tuwien.ac.at, <sup>b\*</sup>roland.haubner@tuwien.ac.at

**Keywords:** San Mai steel; composite steel; forging; diffusion.

### Abstract.

In the context of a knife blade, the term San Mai is used for the manufacture of a usually three layered steel composite. The middle layer, which forms the cutting edge, consists of hard steel and on the outside a soft stainless steel is forged. Mr. Benjamin Kamon, an Austrian blacksmith, provided the examined sample.

Three different steels and a thin Ni layer are symmetrically connected (1.4301/1.3520/Ni/1.2519/Ni/1.3520/1.4301) (Fig. 1a, b). The middle layer is a cold work steel (1.2519) and the Ni layer is to prevent diffusion processes. 1.3520 is a heat treatable steel for rolling bearings, followed by an austenitic stainless steel (1.4301).

Fig. 1c shows an overview of the existing interfaces. All layers are well connected and no defects are evident. Fig. 1d shows the hardened microstructure of the steel 1.2519, Fig. 1e shows the diffusion of C in the austenitic steel and carbide formation at the grain boundaries and in Fig. 1f and 1g the coarse-grained Ni layer can be seen. Hardness profiles were also measured and diffusion profiles between the different steels were analyzed using SEM-EDX.

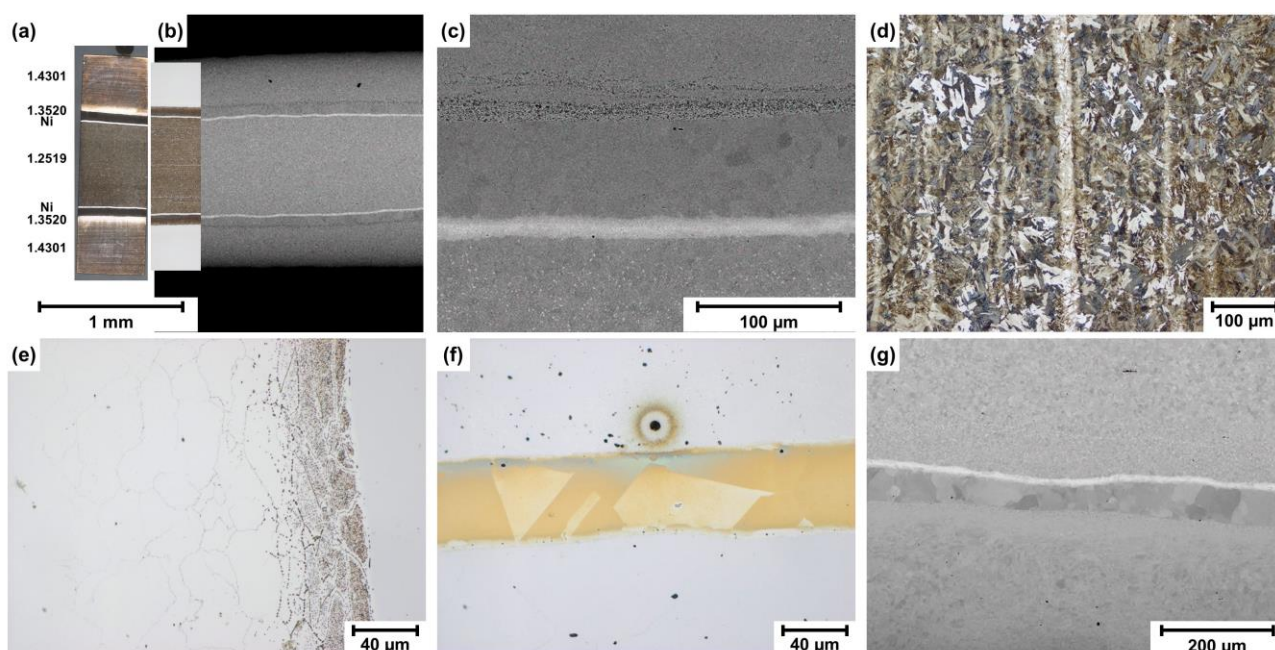


Fig. 1 (a) cross section in LOM, (b) cross section in SEM, (c) detail of the different interfaces in SEM, (d) 1.2519, Nital etched, (e) interface 1.3520/1.4301 showing carbon diffusion and carbide formation in the austenitic steel (Murakami etch), (f) Ni layer etched with Lichtenegger Bloech, (g) Ni layer in SEM.

## Microstructure and Fatigue Behavior of High Performance Aluminum Alloy Al2024 Produced by Laser Powder Bed Fusion

Konečná Radomila<sup>1,a\*</sup>, Varmus Tibor<sup>1,b</sup>, Federico Uriati<sup>2,c</sup>  
and Gianni Nicoletto<sup>2,d</sup>

<sup>1</sup>University of Zilina, Univerzitná 1, 01026 Zilina, Slovakia

<sup>2</sup>University of Parma, Parco Area delle Science 181/A, Parma, Italy

<sup>a\*</sup>radomila.konecna@fstroj.uniza.sk, <sup>b</sup>tibor.varmus@fstroj.uniza.sk, <sup>c</sup>federico.uriati@unipr.it,  
<sup>d</sup>gianni.nicoletto@unipr.it

**Keywords:** Al2024; L-PBF; fatigue; microstructure.

### Abstract.

Aluminum-based alloys are widely used in high-performance structural applications. Therefore, the opportunity to fabricate aluminum components using Laser Powder Bed Fusion (L-PBF) is a matter of great interest. In particular, the Al2024 alloy is extensively used for conventional part production but its processability by L-PBF remains a challenge because of its cracking sensitivity upon solidification. Elementum's new Reactive Additive Manufacturing (RAM) technology enables the production of innovative powders characterized by metal matrix and nanoceramic particles that can be processed using L-PBF. The ceramic nanoparticles of 2 % by weight instantly improves properties and prevents Al2024 RAM2 alloy cracking during solidification.

The present study investigates the fatigue performance of Al2024 RAM2 alloy manufactured by L-PBF using an SLM 280 HL fabrication equipment with a nominal layer thickness of 60  $\mu\text{m}$ . A set of miniature vertical fatigue specimens were manufactured then underwent a solution plus aging heat treatment (T6). The specimens were tested in the as-built state (i.e. without any surface post-processing) under cyclic plane bending at a load ratio  $R = 0$  at a frequency of 25 Hz. The fatigue performance was determined and compared to that of other Al-alloys produced by L-PBF. Specimens were examined by using light microscopy analysis to determine the microstructure shown in Fig. 1a. The fracture surfaces of vertical specimens were investigated in the SEM to determine the mechanisms of crack initiation (Fig. 1b).

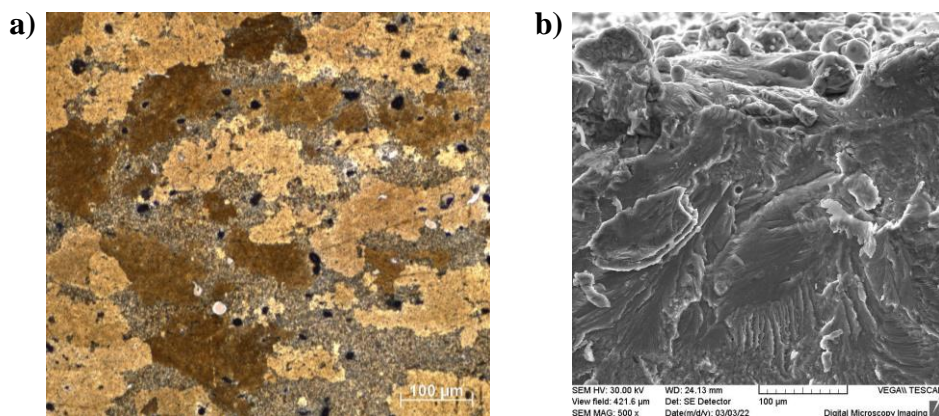


Fig. 1 a) Microstructure of vertical specimen, b) Initiation site of fatigue crack.

### Acknowledgments

The authors acknowledge the company BEAM-IT srl, Fornovo Taro, Italy for providing the specimens and the VEGA grant agency for the support by the grant No. 1/0463/19.

## High-Temperature Low Cycle Fatigue of Nickel-Based Superalloy IN738LC

Šulák Ivo<sup>1,a\*</sup>, Chlupová Alice<sup>1,b\*</sup> and Obrtlík Karel<sup>1,c</sup>

<sup>1</sup>Institute of Physics of Materials, Academy of Sciences of the Czech Republic,  
Žižkova 22, 616 00 Brno, Czech Republic

<sup>a</sup>sulak@ipm.cz, <sup>b</sup>chlupova@ipm.cz, <sup>c</sup>obrtlik@ipm.cz

**Keywords:** superalloy IN738LC; microstructure; fatigue; fractography.

### Abstract.

Polycrystalline cast nickel-based superalloy IN738LC is employed for critical parts of gas turbine components in the power industry, aircraft engines, and the marine sector. These components undergo severe degradation by low cycle fatigue caused by thermal gradients, particularly during start-ups and shut-down periods. The present work reports the cyclic deformation behaviour and fatigue damage of IN738LC during high-temperature isothermal fatigue. Cylindrical specimens were cyclically deformed under strain control with constant total strain amplitude in symmetrical cycling at 800°C, 900°C, and 950°C in air. The microstructure (see Fig. 1a) is typical of coarse dendritic grains with carbides, eutectic and shrinkage pores. SEM imaging revealed  $\gamma$  matrix with coherent L12  $\gamma'$  precipitates with bimodal morphology. Cyclic hardening/softening curves, cyclic stress-strain response and fatigue life diagrams were determined. An increase in testing temperature is associated with a significant decrease in stress amplitude and an increase in plasticity. The fatigue life gradually decreases with increasing temperature. The fracture surfaces (see Fig. 1b) and polished sections parallel to the specimen axis were examined to study damage mechanisms in cyclic loading at high temperatures.

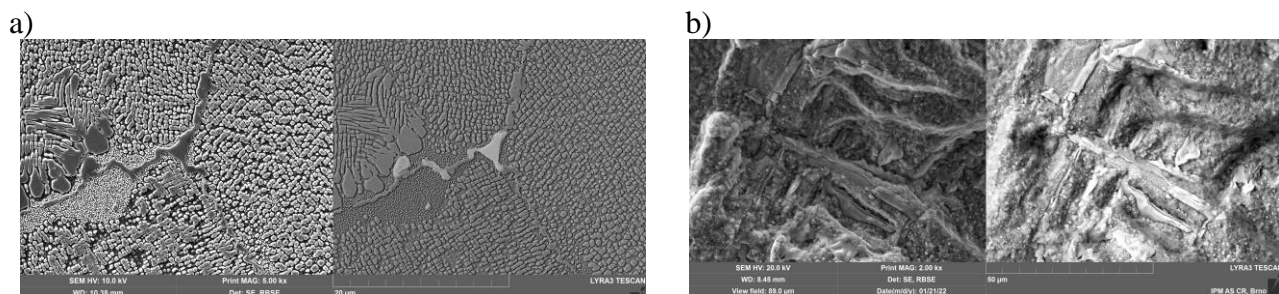


Fig. 1 SEM micrographs of microstructure (a) and fracture surface (b) of IN738LC.

### Acknowledgment

Project FW03010190 (TAČR Trend) is acknowledged.

## Investigation of Fatigue Failure in Electric Locomotive Axle

Pytel Stanisław

Institute of Technology, State University of Applied Sciences,  
ul. Zamenhofa, 33-300 Nowy Sącz, Poland

spytel@pwsz-ns.edu.pl

**Keywords:** electric locomotive axle; padding weld; fatigue damage; metallographic and fractographic examinations.

### Abstract.

The main goal of this work was to conduct laboratory tests of the steel applied in the electric locomotive axle in accordance with the PN-93/K-9146 standard and then to determine the cause of its fatigue damage. In the first stage the chemical composition and mechanical properties tests as well as observations of the macro and microstructure of the axle material were carried out. Based on the results obtained in first stage, it can be concluded that the axle was made of non-alloy structural steel with an average carbon content. The obtained results are referred to the conditions contained in the PN-91/H-84027/3 standard for steel P35G. It should be noted that the axle material meets all the requirements contained in the normative documents.

The second stage of the study was devoted to metallographic and fractographic studies, the purpose of which was to determine the cause and mechanism of axle damage. The scrap was formed in the transition radius zone between the axis resting pin and the central part. Scrap is typical of a variable bending and rotational load, with a clearly located focus and a proximity zone. Detailed observations of the microstructure using a scanning electron microscope (SEM) showed that the P35G steel used for the production of axle has a fine grained ferritic-perlitic microstructure with a small content of elongated manganese sulfides.

Detailed fractographic studies showed that the direct cause of the catastrophic fracture of the axle was a padding weld with a depth about 3 mm made on the surface of the axle. In addition, it was clearly confirmed by the results of microhardness measurements in the weld region that the hardness of the steel was at least twice as high as the hardness of the base material (HV230) versus (HV600 ÷ HV400). Very large difference in the hardness of the heat affected zone of weld and the axle material, most likely due to the high cooling rate during the padding process. This must have caused significant thermal and structural stresses. According to the fractographic analysis performed by SEM, these several millimeter cracks were the direct cause of the gradual spread of the fatigue failure. Detailed studies of the fracture surface were impossible due to the significant mechanical destruction of this surface.

## Analysis of Cracks of Thermostats Casings Made of Brass

Kasl Josef<sup>1,a\*</sup>, Aišman David<sup>1,b</sup> and Fikrlová Růžena<sup>1,c</sup>

<sup>1</sup>VZÚ Plzeň, Tylova 1108/46, 301 00 Plzeň, Czech Republic

<sup>a\*</sup>kasl@vzuplzen.cz, <sup>b</sup>aisman@vzuplzen.cz, <sup>c</sup>fikrlova@vzuplzen.cz

**Keywords:** thermostat; failure; microstructure; fractography; stress corrosion cracking.

### Abstract.

As part of the project “Thermostat for universal use in (electro) mobility”, an analysis of three failed thermostats after operation was performed. The principle of the thermostat is based on the phase transformation of wax in the closed volume of the thermostat, during which the piston is pushed out and the valve is opened. The thermostat, in addition to the wax filling, the steel piston and the rubber seals, consists of a casing and a piston guiding, which are made of brass. Two variants of the thermostat were evaluated. In one case, the casing and the guide element were made of CuZn39Pb3 alloy, in the other two ones the casing was made of CuZn36 alloy. Thermostats also differed in shape. Cracks always occurred on the casings. In the first case, crack occurred at the "bottom" of the casing, in the second two on the casings at the location of the guiding elements. The maximum operating temperature was up to 100 ° C; operating time / mileage data were not available.

The cracks were open and fractographical observation was performed. The microstructure of the material was evaluated using both the light and scanning electron microscopy. The local composition of the material was determined by EDS microanalysis. Furthermore, micro-hardness profiles were measured.

In the first case, there was a network of branching cracks initiated on the curved outer surface of the casing. The cracks were predominantly intergranular; however, the facets of transgranular cleavage were present too (Fig. 1). The microstructure was formed by a mixture of  $\alpha$ - and  $\beta$ -phase and lead particles. In the other two cases, the cracks were similar. Cracks were initiated on the outer surface in the area of the fastening of the guiding. The crack propagated both in the intergranular and transgranular way. The size of the facets varied depending on the amount of deformation of the wall material. The microstructure consisted of a mixture of  $\alpha$ - and  $\beta$ -phases with different grain sizes. In addition to the stress caused by the overpressure of the molten wax, a higher level of residual stresses caused by deformations can be expected in the places where the thermostat is calibrated or where the guiding is pressed into the casing (i.e., at the crack positions). The failure was caused by the mechanism of stress-corrosion cracking. Metal induced embrittlement could interact in the first case or corrosion fatigue in the second two ones.

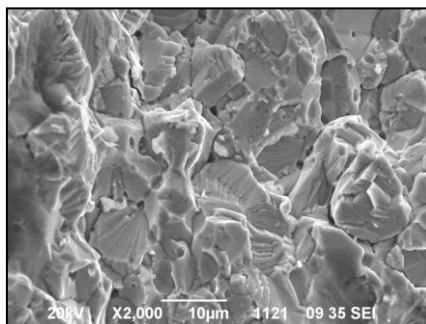


Fig. 1 Fracture surfaces of crack.

### Acknowledgment

This work has been carried out in the frame of the project TREND FW03010487 with financial support from the Technology Agency of the Czech Republic.

## Structure and Properties of FeGaX (X=Tb, Y) Alloys

Milyutin Vasily<sup>1,a</sup>, Bureš Radovan<sup>1,b</sup>, Fáberová Mária<sup>1,c</sup>  
and Birčáková Zuzanna<sup>1,d</sup>

<sup>1</sup>Institute of Materials Research, Slovak Academy of Sciences,  
Watsonova 47, 040 01 Kosice, Slovak Republic

<sup>a</sup>\*vmilyutin@saske.sk, <sup>b</sup>rbures@saske.sk, <sup>c</sup>mfaberova@saske.sk, <sup>d</sup>zbircakova@saske.sk

**Keywords:** Fe-based alloys; soft magnetic materials; magnetic properties; magnetostriction.

### Abstract.

Since 2000 Fe-Ga binary alloy is an object of increased interest due to abnormally high magnetostriction. The most widespread composition is Fe-19 at. % Ga in addition to high magnetostriction has a combination of other useful properties. In recent years, work has been carried out on alloying the binary alloy with a small amount of rare-earth elements, which makes it possible to increase the functional characteristics of the alloy [1]. Magnetostrictive materials are used in different devices and sensors, some of which operate at elevated frequencies of magnetization reversal. The structure and properties of  $\text{Fe}_{81}\text{Ga}_{19}$ ,  $(\text{Fe}_{81}\text{Ga}_{19})_{99.8}\text{Tb}_{0.2}$ , and  $(\text{Fe}_{81}\text{Ga}_{19})_{97}\text{Y}_3$  alloys have been studied in this work; many of the results have been obtained for the first time. For example, electrical resistivity and frequency stability of the magnetic permeability of FeGaRE alloys, which are extremely important for operation at elevated frequencies (Table 1). The structure of doped alloys is shown in Fig.1. Rare-earth elements have very limited solid solubility in  $\alpha$ -iron lattice and form Tb- and Y-rich phases, mainly located along grain boundaries.

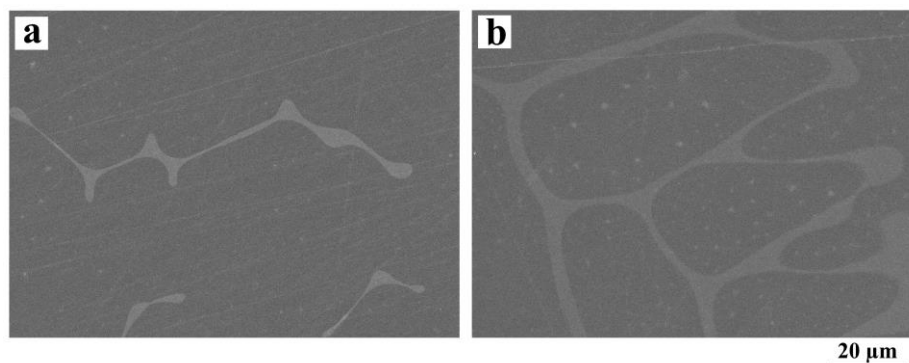


Fig. 1. Structure of  $(\text{Fe}_{81}\text{Ga}_{19})_{99.8}\text{Tb}_{0.2}$  (a) and  $(\text{Fe}_{81}\text{Ga}_{19})_{97}\text{Y}_3$  (b) at magnification x1000.

Table 1 The real part of permeability ( $\mu$ ), coercivity ( $H_C$ ), and electric resistivity ( $\rho$ ) of samples

	$\mu$ (real part) at 1 kHz	$H_C$ , A/m	$\rho$ , $\mu\Omega$ cm
$\text{Fe}_{81}\text{Ga}_{19}$	171.2	120.7	103
$(\text{Fe}_{81}\text{Ga}_{19})_{99.8}\text{Tb}_{0.2}$	107.1	138.2	150
$(\text{Fe}_{81}\text{Ga}_{19})_{97}\text{Y}_3$	106.7	146.3	139

### Acknowledgment

The research was supported by Mobility and Reintegration Programme of the Slovak Academy of Sciences (MoRePro) number 19MRP0061.

### References

[1] Y. He, C. Jiang, W. Wu, B., et. al, Giant heterogeneous magnetostriction in Fe-Ga alloys: Effect of trace element doping, *Acta Mater.* 109 (2016) 177–186.

## Microstructure-Properties Characterization of Selective Laser Melted Biomedical Co-28Cr-6Mo Alloy

Efremenko Bohdan<sup>1,a</sup>, Zurnadzhy Vadym<sup>2,b</sup>, Chabak Yuliia<sup>2,c</sup>,  
Lekatou Angeliki G.<sup>3,d</sup>, Hornak Peter<sup>4,e</sup>, Vojtko Marek<sup>5,f</sup>  
and Efremenko Vasily<sup>2,g\*</sup>

<sup>1</sup>Pryazovskyi State Technical University, Department of Biomedical Engineering,  
Mariupol, 87555, Ukraine

<sup>2</sup>Pryazovskyi State Technical University, Department of Physics, Mariupol, 87555, Ukraine

<sup>3</sup>University of Ioannina, Department of Materials Science and Engineering,  
45110, Ioannina, Greece

<sup>4</sup>Faculty of Materials, Metallurgy and Recycling, Technical University of Kosice,  
042 00 Kosice, Slovakia

<sup>5</sup>Slovak Academy of Sciences, Institute of Materials Research, 040 01 Kosice, Slovakia

<sup>a</sup>efremenko\_b\_v@pstu.edu, <sup>b</sup>zurnadzhy\_v\_i@pstu.edu, <sup>c</sup>julia.chabak25@gmail.com,  
<sup>d</sup>alekatou@uoi.gr, <sup>e</sup>peter.hornak@tuke.sk, <sup>f</sup>mvojtko@saske.sk, <sup>g</sup>vgefremenko@gmail.com

**Keywords:** Co-28Cr-6Mo alloy; selective laser melting; microstructure; nanoindentation; sliding wear.

### Abstract.

Co-28Cr-6Mo alloy (ASTM F75) is widely used in different biomedical applications (dental devices, orthopedic implants, etc.). Casting and metal forming are the two conventional technologies for the fabrication of this alloy. Recently, additive manufacturing has also been adopted. Due to the peculiarities of this technological process, 3D-printed alloys differ from traditionally manufactured alloys in their structure and properties. In the present work, the features of selective laser melted Co-28Cr-6Mo alloy were studied in comparison with its wrought analogue. The study included microstructural characterization (optical and electron scanning microscopy), nanoindentation, and tribological testing. It was shown that the Selective Laser Melted (SLM) alloy featured the “fish-scale” structure, characteristic of additively fabricated alloys. This structure was composed of fine columnar dendrites. SLM Co-28Cr-6Mo was found equivalent or superior to the wrought alloy in terms of properties, such as hardness, elastic modulus and tribological behavior that makes SLM Co-28Cr-6Mo a promising candidate for implant applications.

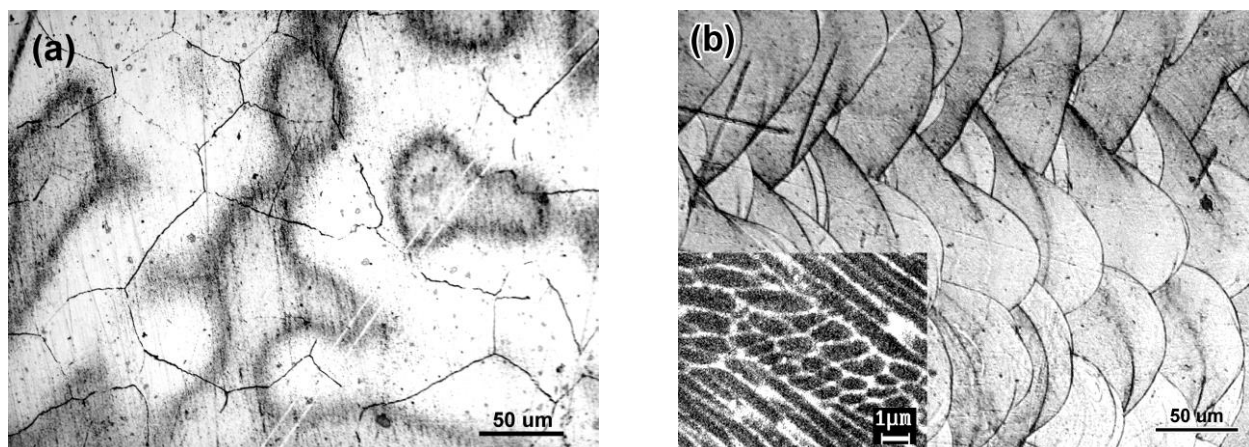


Fig. 1 Microstructure of Co-28Cr-6Mo alloy: (a) wrought; (b) SLM-printed.

## Numerical Simulation of the Welding Process During the Main Circulation Pump Impeller Repair

Baláž Milan

Welding Research Institute, Račianska 71, 83102 Bratislava, Slovakia

balazm@vuz.sk

**Keywords:** numerical simulation of the welding process; main circulation pump impeller; finite element method; stress-strain analysis; residual stresses.

### Abstract

Paper presents a numerical simulation of the welding process during the main pump impeller damaged parts repair for the prediction of welding-induced residual stresses. 3D numerical models creation of the impeller flange and central hub welded joints. Thermal and stress-strain analysis of assessed parts using the finite element method. Calculation of equivalent residual stresses in the area of examined welded joints. Applicability of results in further impeller integrity analyzes. The results confirm the suitability of the chosen welding procedure and technology.

### Acknowledgment

Paper was prepared with the support of the EFRR under the Operational Program Research and Innovation, project number 313021W996 "*Research of corrosion and corrosion cracking in the pressure systems of the primary circuit of nuclear power plants*".

## Technology Influence on the Quality of Cladding Layers

Viňáš Ján<sup>1,a\*</sup>, Brezinová Janette<sup>1,b</sup>, Brezina Jakub<sup>1,c</sup> and Sailer Henrich<sup>1,d</sup>

<sup>1</sup>Technical University of Košice, Faculty of Mechanical Engineering, Košice, Slovakia

<sup>a\*</sup>jan.vinas@tuke.sk, <sup>b</sup>janette.brezinova@tuke.sk, <sup>c</sup>jakub.brezina@tuke.sk, <sup>d</sup>henrich.sailer@tuke.sk

**Keywords:** renovation layers; laser; TOP TIG; casting of aluminium; molds.

### Abstract.

Experimental work was focused on the restoration of functional surfaces of shaped parts of molds for high-pressure casting of aluminum alloys. Paper presents the results of research aimed at determining the quality of renovation layers applied by laser technology and TOP TIG technology. The TruDisk 4002 solid-state disk laser and the AirLiquide TOPTIG 220 cladding power source were used to create the clads. Clad was applied to the base material of nickel-chromium-molybdenum vanadium steel 1.2714, DIN-56NiCrMoV7, with a hardness of 44 HRC. Uddeholm Deivar 1.2344, DIN - X40CrMoV51 additive material in form of wire with a diameter of 1.2 mm was used. The quality of the clads were evaluated using light and electron microscopy and EDX microanalysis. The size of the HAZ and the presence of internal defects in the clads were determined. Value of HAZ was set as max. a min.. Experimental work was supplemented by evaluation of tribological properties of clads by Pin-on-disc method [1].

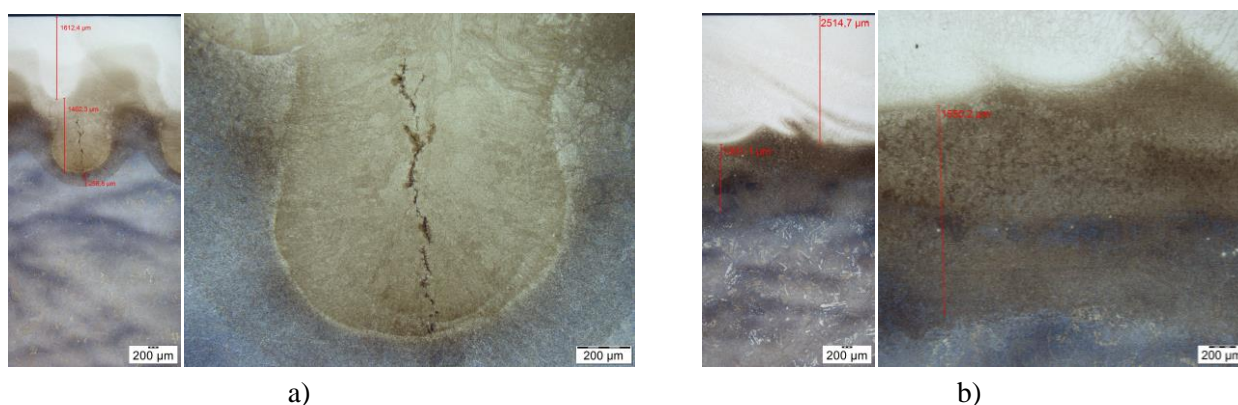


Fig. 1 Appearance of the structure of welds applied a) by laser, b) by TOPTIG technology

### Acknowledgment

This contribution is the result of the project implementation: “Innovative approaches to the restoration of functional surfaces by laser weld overlaying” (APVV-20-0303), supported by the Slovak Research and Development Agency and supported by the Ministry of Education of Slovakia Foundation under grant projects VEGA No. 1/0497/20 “Application of progressive technologies in restoration of functional surfaces of products”.

### References

- [1] K. Bobzin, T. Brögelmann, R.H. Bruognara, N.C. Kruppe: CrN/AlN and CrN/AlN/Al<sub>2</sub>O<sub>3</sub> coatings deposited by pulsed cathodic arc for aluminum die casting applications. *Surface & Coatings Technology* 284 (2015) 222–229.

## Carbon Fibers Doped by Binary Phosphides as an Electrocatalytic Layer for PEM Electrolysers

Bera Cyril<sup>1,2,a</sup> and Strečková Magdaléna<sup>2,b</sup>

<sup>1</sup>Institute of Materials Research, Slovak Academy of Sciences,  
Watsonova 1935/47, Košice, Slovakia

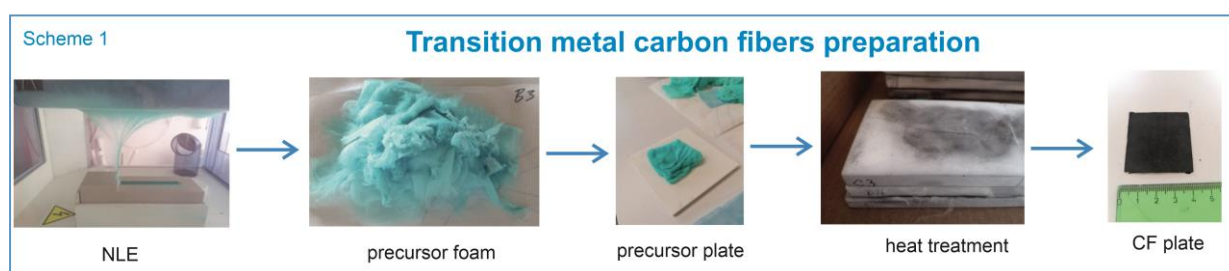
<sup>2</sup>Faculty of Materials, Metallurgy and Recycling, Technical University of Košice,  
Letná 9, Košice, Slovakia

<sup>a</sup>cyril.bera@tuke.sk, <sup>b</sup>mstreckova@saske.sk

**Keywords:** carbon fibers; electrocatalytic layer; electrolysers; hydrogen evolution reaction.

### Abstract.

The hydrogen evolution reactions (HER) play a decisive role in a range of electrochemical devices such as electrolysers or fuel cells. It is necessary to develop an efficient, low cost and robust electrocatalysts to lower the reaction overpotential and minimize energy consumption. The three different electrocatalysts were prepared by needle-less electrospinning (NLE) technology according to Scheme 1. NLE represent user friendly and versatile technology for low-cost fibers production in large scale. Transition metal phosphides (TMP) carbon fibers (CF): NiCoP CF, FeNiP CF and FeCoP CF with different bimetallic incorporated nanoparticles into carbon fibers were prepared by NLE and followed by optimized heat treatment process. The precursor fibers were obtained in the form of polymeric foam and subsequently folded between two Al<sub>2</sub>O<sub>3</sub> ceramic plates. The heat treatment was realized in the tubular furnace in Ar atmosphere at 1200 °C and followed by the reduction H<sub>2</sub> atmosphere at 780 °C. The final TMP CF in the form of plates can be directly immersed to the membrane electrode assembly of electrolyzer in Figure 1. The electrochemical activity of the prepared electrocatalysts was measured by linear sweep voltammetry in the three-electrode set up. The stability and durability of the catalyst was studied in acidic and alkali environment.



Scheme 1 Transition metal carbon fibers preparation.

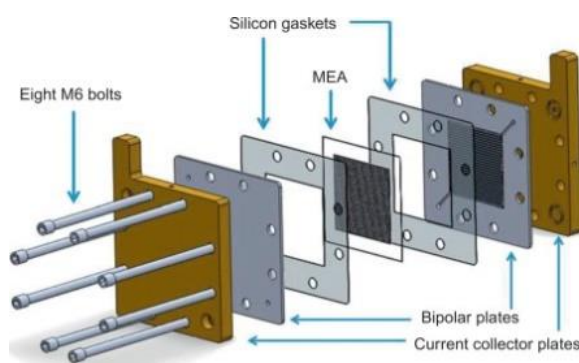


Fig. 1 Membrane electrode assembly.

## Application of Copper Powder in Manufacturing of Composite Filament in 3D Printings

Dzindziora Agnieszka<sup>1,a\*</sup>, Dzienniak Damian<sup>1,b</sup> and Sułowski Maciej<sup>1,c</sup>

<sup>1</sup>AGH University of Science and Technology in Kraków, Poland

<sup>a\*</sup>dzindziora@agh.edu.pl, <sup>b</sup>ddamian@agh.edu.pl, <sup>c</sup>sulek@agh.edu.pl

**Keywords:** PLA; 3D printing; copper filament; printed composite.

### Abstract.

The aim of the experimental research was to produce a filament based on PLA plastic with the admixture of various concentrations of copper.

To produce the filament with copper admixtures, a specialized precise extruder was used, which allows the preparation of a composite filament based on plastics. The base component was a PLA thermoplastic polymer belonging to the group of aliphatic polyesters. The created composite structure was intended for 3D printing using the FDM method (Fused Deposition Modeling).

The type of granules used to produce the filament has a significant impact on the quality of the product. The additions of various substances introduced into the filament determine its properties. Many of the parameters influencing the filament manufacturing process, such as the process temperature, the drop in ambient temperature during the cooling and stabilization of the filament, material moisture and air humidity, have not been sufficiently studied.

Composites based on PLA and copper have different properties from pure PLA.

## Optimization of Raster Point Deposition Methodology for Deformation Analyses

Duchac Alfred<sup>1,2,a\*</sup> and Kejzlar Pavel<sup>2,b</sup>

<sup>1</sup>Centrum výzkumu Řež s.r.o. , Hlavní 130, 250 68 Husinec – Řež, Czechia

<sup>2</sup>Technical University of Liberec, Studentska 1402/2, 461 17 Liberec, Czechia

<sup>a\*</sup> alfred.duchac@cvrez.cz , <sup>b</sup> pavel.kejzlar@tul.cz

**Keywords:** deformation analyses; hot-dip galvanized metal sheets; point pattern deposition; microstructure analysis.

### Abstract.

Deformation analysis of sheet metal parts helps to map the distribution of deformation zones during pressing in problematic areas of the car bodywork. This helps solve and prevent production problems at the press shop. The present work is focused on the optimization of the process by point pattern deposition on hot-dip galvanized metal sheets for deformation analyses. Obtained data are evaluated by GOM Argus system. Two technologies of the pattern deposition, namely electrochemical and laser are compared. Both deposition methods behave differently in the forming process and show different deformation values. The microstructure analysis by a scanning electron microscope shows that the influence of laser setting on the material is more significant compared to electrochemical etching, Fig.1. Laser material shows thermal influence on the base material and the formation of micro notches. Both technologies are compared using light optical microscopy, scanning electron microscopy, energy-dispersive analysis and electron backscattered diffraction.

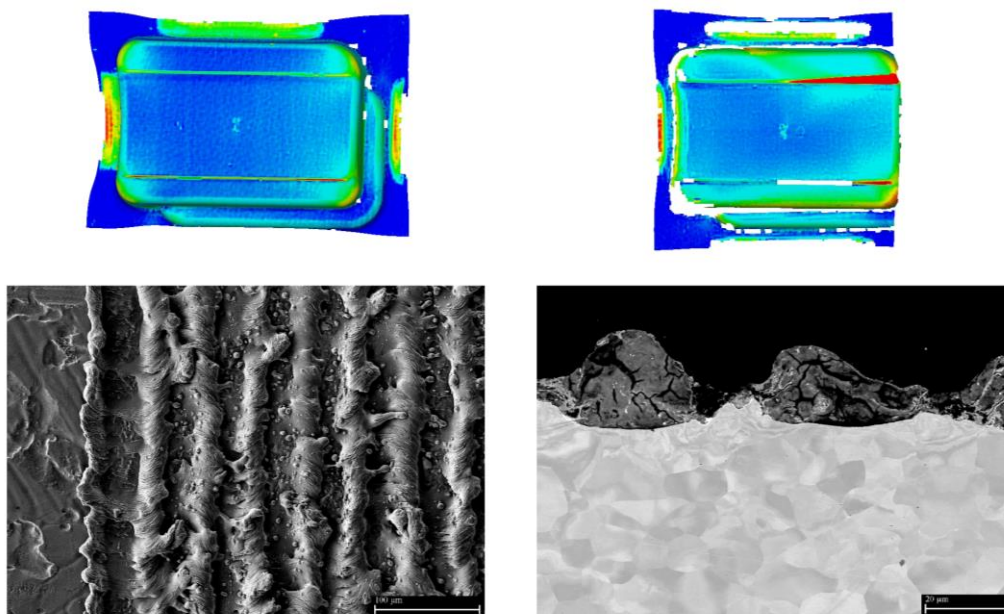


Fig. 1 Comparison of deformation analysis and influence due to thermal influence of base material with indentations.

### Acknowledgement

The publication was created in Research Centre Řež within Institutional Support by Ministry of Industry and Trade of the Czech Republic and was also written at the Technical University of Liberec, Faculty of Mechanical Engineering with the support of the Institutional Endowment for the Long Term Conceptual Development of Research Institutes, as provided by the Ministry of Education, Youth and Sports of the Czech Republic in the year 2022.

# **POSTER PRESENTATIONS**

## Automation of Metallographic Sample Etching Process

Ambrož Ondřej<sup>1,a\*</sup>, Čermák Jan<sup>1</sup>, Jozefovič Patrik<sup>1</sup> and Mikmeková Šárka<sup>1</sup>

<sup>1</sup>Institute of Scientific Instruments of the CAS, Královopolská 147, 612 00 Brno, Czech Republic

<sup>a\*</sup>ondrej@isibrno.cz

**Keywords:** metallography; chemical etching; process automation; repeatability; robotics.

### Abstract.

Chemical etching is an integral part of metallographic sample preparation. Maintaining precise etch times can be difficult and therefore repeatability is limited. The aim of this work is to improve the repeatability of sample preparation using robotization.

Prior to etching, metallographic samples of S355J2 (1.0577) structural steel were finely mechanically polished. For verification, 15 specimens were prepared using an in-house designed automated etching machine with a built-in 5-axis robotic arm and 15 specimens prepared manually by an expert metallographer. The samples were etched with Kourbatoff no. 4 reagent for 8 seconds in a beaker placed in an ultrasonic cleaner at 80 kHz. The samples were then cleaned in 7 beakers of cleaning fluid also placed in the ultrasonic cleaner.

The robotic etching and cleaning process was optimized and the quality of the resulting surface is at least as good as that of the samples prepared by an expert metallographer. The surfaces were compared using a light optical microscope (LOM) and a confocal laser scanning microscope (CLSM).

The repeatability of the preparation process is a key aspect for obtaining a large dataset of steel microphotographs for training a deep neural network that will be used in future research.

## Identification of Corrosion Mechanisms of Stainless Steel with Metallography Cross Sections

Geiplova Hana<sup>1,a\*</sup>, Vlachova Marketa<sup>1,b</sup> and Piskova Anna<sup>1,c</sup>

<sup>1</sup>SVUOM Ltd., U Mestanskeho pivovaru 934/4, 170 00 Prague 7, Czech Republic

<sup>a</sup>geiplova@svuom.cz, <sup>b</sup>vlachova@svuom.cz, <sup>c</sup>piskova@svuom.cz

**Keywords:** stainless steel; heat exchanger; chemical composition; localised corrosion mechanisms; tube sheet.

### Abstract.

Stainless steel X6CrNiTi18-10 (1.4541, AISI 321) is the basic austenitic iron-based alloys that contain nominally 19% chromium and 9% nickel with Ti contain as stabilizing element. The metallography was used for evaluation of localized form of corrosion of stainless steel tubesheets of heat exchangers. The heat exchangers were in service for relative short period from few months to 2 years. The service conditions of these heat exchangers were different (temperature, medium, etc.) and caused penetration of tube walls. The metallography cross sections were used to identified the corrosion mechanisms – Fig. 1. For all evaluated cases the different mechanisms were found – pitting corrosion and intercrystallite corrosion cracking due to sulphide content in oil deposits (sample 1), trans-crystalline corrosion cracking due to overheating caused by water scale deposits (sample 2) and microbially induced corrosion under slime layer (sample 3). Together with X ray diffraction and elementary analysis of corrosion products the metallography evaluation was used for identification of corrosion mechanisms.

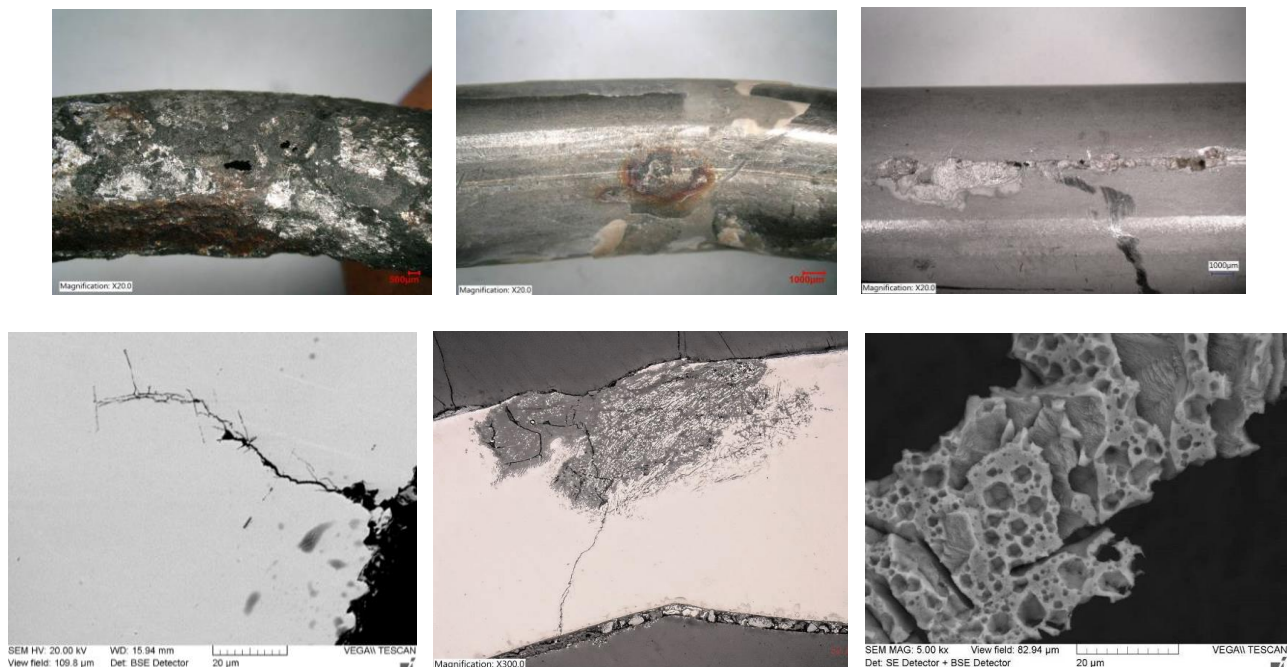


Fig. 1 Typical surface conditions of corroded tubes and microscopy images illustrate corrosion mechanisms.

### Acknowledgment

The study was performed and paper was written with support of project MPO - IP DKRVO, 2021.

## Highly Accurate Structural Analysis of Austempered Ductile Iron Using EBSD Technique

Kejzlar Pavel<sup>1,a\*</sup>, Andrsova Zuzana<sup>1,b</sup>, Petrzkova Michaela<sup>1,c</sup>,  
SkrbekBretislav<sup>1,d</sup> and Myszka Dawid<sup>2,e</sup>

<sup>1</sup>Technical University of Liberec, Studentska 1402/2, 461 17 Liberec, Czechia

<sup>2</sup>Faculty of Production Engineering, Warsaw University of Technology,  
Ludwika Narbutta 85, 02-524 Warszawa, Poland

<sup>a\*</sup>pavel.kejzlar@tul.cz, <sup>b</sup>zuzana.andrsova@email.cz, <sup>c</sup>michaela.petrzkova@tul.cz,  
<sup>d</sup>bretislav.skrbek@tul.cz, <sup>e</sup>dawid.myszka@pw.edu.pl

**Keywords:** austempered ductile iron; EBSD; structure; phase analysis; heat treatment.

### Abstract.

ADI (Austempered Ductile Iron) is characterized by a favourable combination of ductility and strength, which exceeds most of heat-treated carbon steels in the range of 800 to 1500 MPa. Isothermal hardening used for their production causes the formation of a fine dispersion of epitaxial ferrite and residual austenite, the so-called ausferrite. The heat treatment parameters directly affect the ausferrite structure, which affects its mechanical properties; e.g., the finer the slats, the higher the mechanical strength. At the same time, the more austenite the structure contains, the higher its ductility. It is challenging to characterize this very fine structure satisfactorily using conventional methods like optical or scanning electron microscopy. Thus EBSD has been used for this purpose. The EBSD method provides data about the crystal structure and its orientation enabling the processing of the obtained data through various maps (phase, orientation, deformation, etc.), which allows obtaining the necessary information characterizing the material structure.

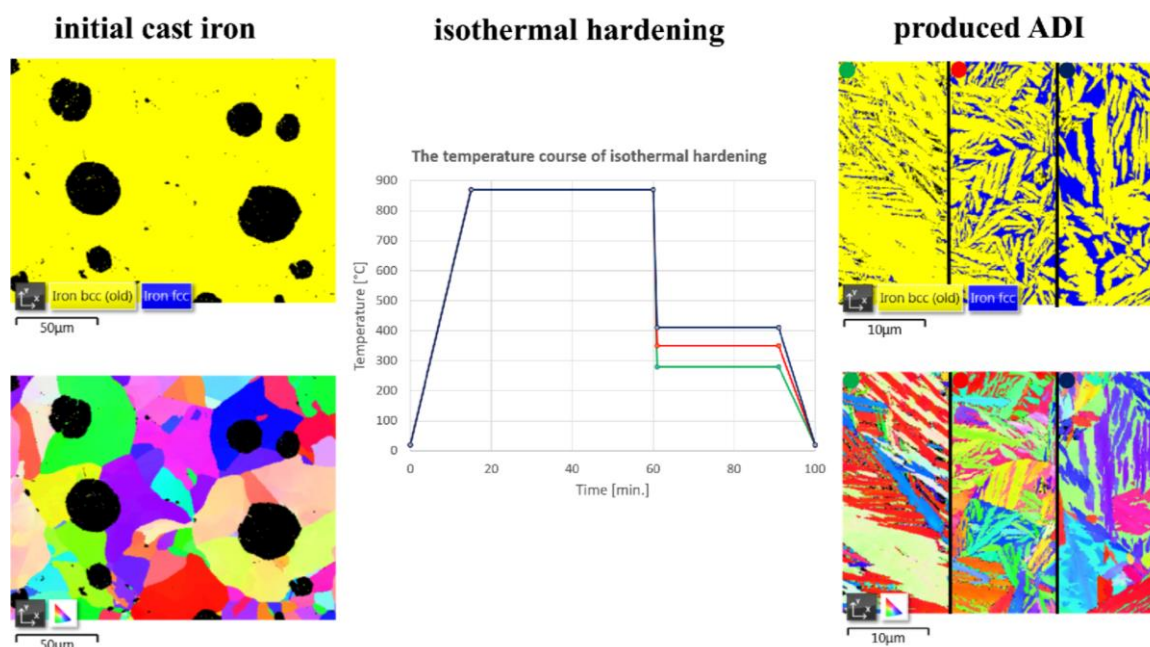


Fig. 1 Structural changes caused by variation of isothermal hardening temperature.

### Acknowledgement

Publishing the results was financially supported by the Ministry of Education, Youth and Sports of the Czech Republic and the European Union in the frame of the project “International Research Laboratories”, Reg. No. CZ.02.2.69/0.0/0.0/18\_054/0014685.

## **A Study of Cut Surface After the Abrasive Water Jet Application on the MS1 Material Prepared by DMLS Method**

Vandzura Radoslav<sup>1,a\*</sup>, Simkulet Vladimir<sup>1,b</sup>, Botko Frantisek<sup>1,c</sup>  
and Gelatko Matus<sup>1,d</sup>

<sup>1</sup>Department of Automobile and Manufacturing Technologies, Faculty of Manufacturing Technologies with a Seat in Presov, Technical University of Kosice, Bayerova 1, 08001 Presov, Slovakia

<sup>a</sup>radoslav.vandzura@tuke.sk, <sup>b</sup>vladimir.simkulet@tuke.sk, <sup>c</sup>frantisek.botko@tuke.sk  
<sup>d</sup>matus.gelatko@tuke.sk

**Keywords:** abrasive water jet; AWJM; DMLS; additive manufacturing.

### **Abstract.**

This contribution deals with the study of cut surface after the abrasive water jet application on the material Maraging Steel MS-1, prepared in the form of 3D printing method Direct Metal Laser Sintering. The aim of the study is to point out the morphology of the cut plane under the use of various technological parameters, like feed rate of machining and abrasive mass flow at the constant cut pressure. For the track morphology monitoring after the abrasive water jet application, scanning electron microscope SEM MIRA 3, f. Tescan, was used. For the identification of observed particles stabbed in the cut track, chemical composition EDX analysis was used.

### **Acknowledgment**

This work was supported by the Slovak Research and Development Agency under the contract No. APVV-20-0514. and KEGA 018TUKE-4/2021.

## Analysis of Tribodegradation Factors Limiting the Life of the Molds

Brezinová Janette<sup>1,a\*</sup>, Miroslav Džupon<sup>2,b</sup>, Viňáš Ján<sup>1,c</sup>, Brezina Jakub<sup>1,d</sup>  
and Hašul' Ján<sup>1,e</sup>

<sup>1</sup>Technical University of Košice, Faculty of Mechanical Engineering, Košice, Slovakia

<sup>2</sup>Slovak Academy of Science, Institute of Materials Research, Košice, Slovakia

<sup>a\*</sup>janette.brezinova@tuke.sk, <sup>b</sup>mdzupon@saske.sk, <sup>c</sup>jan.vinas@tuke.sk, <sup>d</sup>jakub.brezina@tuke.sk,  
<sup>e</sup>jan.hasul@tuke.sk

**Keywords:** aluminum casting; molds; shaped parts; service life; tribology.

### Abstract.

Paper presents the results of research focused on the analysis of mold wear for high-pressure casting of aluminum alloys. Functional parts of the decommissioned molds were analyzed. The mold parts and cores for casting aluminum alloys are made of chrome and chromium molybdenum steel. In the die-casting process, the mold parts and cores are exposed to intense thermal, mechanical and chemical loads. High melt flow rates of aluminum alloys (up to 120 m.s<sup>-1</sup>), high pressures (up to 120 MPa) and high maximum surface temperatures of mold parts (up to 550 °C) lead to erosion, abrasion, corrosion and thermal fatigue of the molds. The thermal load of the foundry cores is even higher (up to 600 °C) because they are not connected to the mold cooling system. Thermal cyclic loading from 80 °C to 550 °C leads to high tensile stresses on the surface of the molded parts / cores and consequently to the formation and propagation of thermal cracks. Frequent contact of the surface of the mold part with the melt causes the formation of growths (sticking) due to corrosion and of influence of molten metals consequently shortens the life of the mold parts and cores. Light and electron microscopy was used for mold analysis. Any degradation change in the shape of molds and cores will also affect the quality and dimensions of the castings [1].

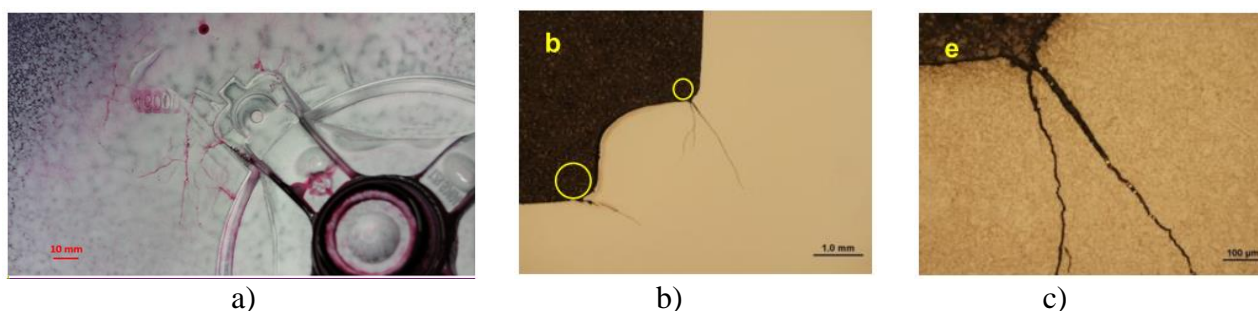


Fig.1 Appearance of shaped parts of molds a), after capillary test b), cracks in areas of sharp surface transitions c).

### Acknowledgment

This contribution is the result of the project implementation: “Innovative approaches to the restoration of functional surfaces by laser weld overlaying” (APVV-20-0303), supported by the Slovak Research and Development Agency and supported by the Ministry of Education of Slovakia Foundation under grant projects VEGA No. 1/0497/20 “Application of progressive technologies in restoration of functional surfaces of products”.

### References

- [1] D. Klobčar, M. Muhič, M. Pleterski, J. Tušek: Thermo-mechanical cracking of a new and laser repair welded die casting die. *Metallurgija* 51 (3) 305-308 (2012).

## Stress–Strain State and Texture Evolution in Cold Drawing of Steel Tubes

Burik Peter<sup>1,a\*</sup>, Bella Peter<sup>1,b</sup> and Kejzlar Pavel<sup>2,c</sup>

<sup>1</sup>ŽP Research and Development Centre, Kolkáreň 35, 976 81 Podbrezová, Slovak Republic

<sup>2</sup>Technical University of Liberec, Institute for Nanomaterials, Advanced Technology and Innovation, Studentská 2, 461 17 Liberec, Czech Republic

<sup>a\*</sup>burik@zelpo.sk, <sup>b</sup>bella@zelpo.sk, <sup>c</sup>pavel.kejzlar@tul.cz

**Keywords:** steel tube; cold drawing; texture; finite element modelling.

### Abstract.

Cold drawing of steel tubes is the manufacturing process characterized by anisotropic material flow during drawing. In order to achieve the final diameter and wall thickness, the input feedstock is progressively reduced in several cold drawing passes. Where both the outer diameter and the wall thickness is to be reduced, fixed plug drawing is used. The final pass to obtain the final outer diameter of the tube is simply the hollow sinking, i.e., drawing without the internal tool. The change in wall thickness during hollow sinking depends on the input dimensions of the tube and also the die geometry [1, 2].

The E235 steel feedstock with given initial dimensions was cold drawn by two different tube drawing processes (fixed plug drawing and hollow sinking). It has been found that the steady state of strain in the tube material during drawing has a significant impact on the change of volume fractions of selected crystallographic orientations. Strain states in selected parts of the tube were described on cylindrical coordinate system for transparent analysis and also for electron backscatter diffraction analysis. A significant difference was detected in the tangential (hoop) direction due to the significant change in wall thickness. Better understanding of this process will make it possible to produce a steel tube with the improved texture to facilitate the cold drawing process.

### References

- [1] P. K. Loharkar, M. K. Pradhan, Modeling and analysis of cold drawing process, Handbook of research on manufacturing process modeling and optimization strategies (2017) 40 - 53.
- [2] H. G. Brokmeier, Texture gradient in a copper tube at maximum and minimum wall thickness, IOP conf. series: Materials science and engineering 82 (2015).

## Formation of Sulphides in As-Cast GOES Thin Strips

Hradečný Kryštof<sup>1,a\*</sup>, Palupčíková Renáta<sup>1,b</sup>, Volodarskaja Anastasia<sup>1,c</sup>  
and Vodárek Vlastimil<sup>1,d</sup>

<sup>1</sup>VSB – Technical University of Ostrava, Faculty of Materials Science and Technology,  
17. listopadu 15, Ostrava – Poruba, Czech Republic

<sup>a\*</sup>krystof.hradecny@vsb.cz, <sup>b</sup>renata.palupcikova@vsb.cz, <sup>c</sup>anastasia.volodarskaja@vsb.cz,  
<sup>d</sup>vlastimil.vodarek@vsb.cz

**Keywords:** GOES; solidification; ( $\delta + \gamma$ ) field; sulphides; Widmanstätten austenite.

### Abstract.

Recent developments in the thin strip casting technology make it possible to apply it for the grain oriented electrical steel (GOES) production. GOES firstly solidifies as  $\delta$  - ferrite, and during following cooling in the ( $\delta + \gamma$ ) field a small amount of austenite and some minor phases precipitate in the ferrite.

This paper deals with the formation of sulphides in as-cast GOES thin strips during solidification and cooling through the ( $\delta + \gamma$ ) field. Thin strips were manufactured using the horizontal belt casting process. In this case, liquid steel flows from a ladle into a tundish system and is dispensed onto a water-cooled belt. The top surface of the solidifying strip is protected by argon. Chemical composition of the strip investigated is given in Table 1. Specimens for microstructure investigations were prepared in the middle width and across the whole thickness of the strip (0.014 m). Microstructural evaluation of as-cast thin strips was carried out by using light microscopy, scanning electron microscopy and transmission electron microscopy.

Table 1 Chemical composition of the GOES strip [wt. %]

C	Si	Mn	S	Cr	Cu	Al
0.034	2.81	0.06	0.024	0.20	0.15	0.002

During solidification coarse sulphides formed especially in the area of final solidification, i.e. at about  $\frac{1}{4}$  depth under the top surface of the strip. These sulphides were rich in iron. Most fine globular precipitates, which formed during cooling of strips in the ( $\delta + \gamma$ ) field, were complex sulphides. These sulphides formed only in ferrite. No precipitation of fine sulphides occurred in austenite due to high solubility of sulphur in austenite. Chemical composition of fine sulphides was variable. Majority of these sulphides were rich in chromium, iron and copper. Electron diffraction studies proved that the crystal structure of fine sulphides was consistent with the  $\text{Cr}_2\text{CuS}_4$  phase. The effect of sulphides on the austenite decomposition at the end of the ( $\delta + \gamma$ ) field was studied. Discontinuous networks of sulphides at ferrite/austenite interfaces made it possible to study the early stages of austenite decomposition. The decomposition of austenite started with the formation of epitaxial ferrite with an identical orientation as the surrounding ferrite.

### Acknowledgment

This paper was created with the contribution of the Doctoral grant competition VŠB TU-Ostrava, reg. no. CZ.02.2.69/0.0/19\_073/0016945 within the Operational Programme Research, Development and Education, under project DGS/TEAM/2020-026 “Study of phase transformations in cast strips GOES”, the projects of Student Grant Competition SP2022/33 “Study of the relationship between the microstructure and properties of progressive technical materials, degradation mechanisms and behaviour of progressive technical materials in different operating conditions” and SP2022/68 “Specific research in the metallurgical, materials and process engineering”.

## The Effect of Improper Post Bend Heat Treatment on Microstructure and Properties of a Pipe Bend Made of 0.5Cr-0.5Mo-0.3V Steel

Kuboň Zdeněk<sup>1,a\*</sup>, Vodárek Vlastimil<sup>2,b</sup> and Rožnovská Gabriela<sup>1,c</sup>

<sup>1</sup>MATERIAL AND METALLURGICAL RESEARCH, Ltd.,  
Pohraniční 693/31, Ostrava Vítkovice, Czech Republic

<sup>2</sup>VŠB – Technical University of Ostrava, Faculty of Materials Science and Technology,  
17. listopadu 15, Ostrava–Poruba, Czech Republic

<sup>a\*</sup>creep.lab@mmvyzkum.cz, <sup>b</sup>vlastimil.vodarek@vsb.cz, <sup>c</sup>gabriela.roznovska@mmvyzkum.cz

**Keywords:** 0.5Cr-0.5Mo-0.3V steel; hot bending; post bend heat treatment; microstructure; secondary phases; stress rupture test.

### Abstract.

Hot bending of creep resistant steels is usually performed above the transition temperature  $A_{c3}$  and comprises a short-term austenitization (typically by induction heating) and bending followed by fast cooling. Especially in case of alloyed steels the austenitization is too short to allow dissolution of special carbides and/or nitrides, which results in the bimodal distribution of them after bending. Therefore, complete post bend heat treatment (PBHT), i.e. normalizing and tempering, must be performed to guarantee the required material properties as well as homogeneous final microstructure.

In order to verify the effect of omitted normalization after bending on the material properties of a pipe bend made of 0.5Cr-0.5Mo-0.3V heat resistant steel, two different heat treatment modes were applied to a pipe sample after a heat cycle simulating hot bending (induction heating and water spray cooling). The first mode was complete PBHT, the second comprised only tempering. Analyses of mechanical properties, microstructure (see Figs. 1 and 2), substructure, as well as stress rupture tests were performed to confirm the effect of PBHT regime on material behaviour.

The sample that was only tempered after bending had higher strength and lower FATT and therefore it virtually could seem to be the preferred one. However, a detailed substructural analysis revealed that particles of the precipitates of secondary phases, which determine the creep resistance of the steels, were coarser and at the same time the density of these particles was significantly lower than in the specimen subjected to complete PBHT. It should be therefore certain that the creep resistance of the specimen only tempered after bending will be adversely affected. However, the stress rupture tests performed at 550 and 575 °C show that the samples after PBHT have lower creep rupture strength, at least in short times to rupture, when the creep properties are controlled also by the initial dislocation density. However, at longer times to rupture this trend changes and the samples after PBHT become more creep resistant.

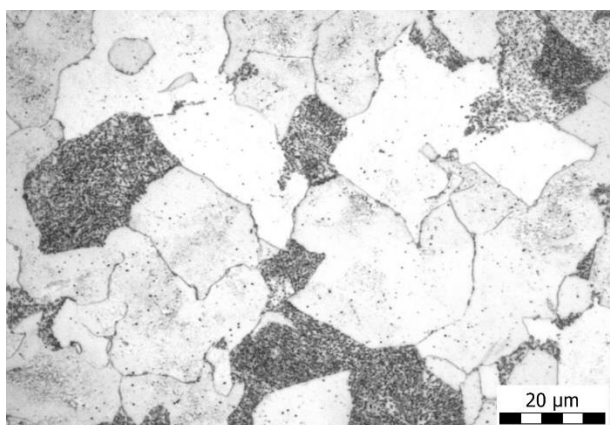


Fig. 1 Microstructure of the steel after PBHT.

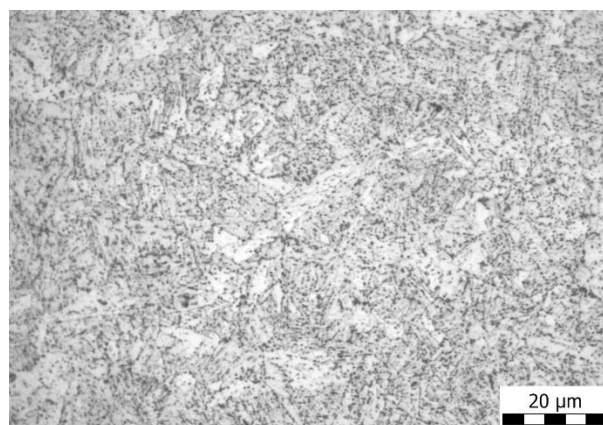


Fig. 2 Microstructure of the only tempered steel.

## Correlation of Magnetic Structural and Mechanical Properties of Selected Classes of Microwires

Milkovičová Jana<sup>1,a\*</sup>, Milkovič Ondrej<sup>1,b</sup>, Hvizdoš Pavol<sup>1,c</sup>, Sedlák Richard<sup>1,d</sup>  
and Csanádi Tamás<sup>1,e</sup>

<sup>1</sup>Slovak Academy of Sciences, Institute of Materials Research,  
Watsonova 47, 040 01 Košice, Slovakia

<sup>a\*</sup>janka.gamcova@gmail.com, <sup>b</sup>omilkovic@saske.sk, <sup>c</sup>phvizdos@saske.sk, <sup>d</sup>rsedlak@saske.sk,  
<sup>e</sup>tcsanadi@saske.sk

**Keywords:** microwires; switching field; diffraction; indentation.

### Abstract.

The aim of presented work is to study the magnetic, mechanical and structural properties of glass-coated magnetic microwires with a nominal composition of FeSiB, FeSiBP and FeSiBPCr. The magnetic properties were evaluated on the basis of the frequency dependences of the critical field. Morphological and structural properties were observed by X-ray diffraction and microanalytical methods. Mechanical properties were estimated on the base of nanoindentation measurements.

Authors correlate the magnetic-mechanical-structural properties of these materials and to propose their use in the field of magnetic sensors.

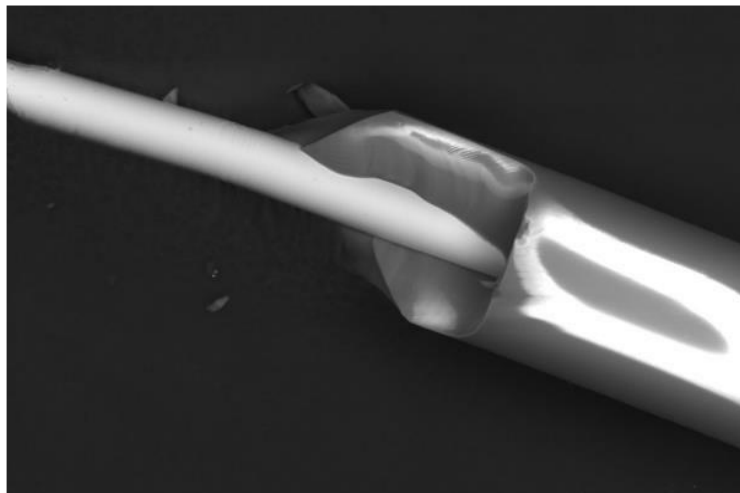


Fig. 1 Microwire Fe<sub>76</sub>Si<sub>9</sub>B<sub>10</sub>P<sub>5</sub>.

## Optimization of the Manufacturing Process of Sintered Fe-Mn-Cr-Mo-C Steels Using ANOVA

Sułowski Maciej<sup>1,a\*</sup>, Matusiewicz Piotr<sup>1,b</sup> and Kij Piotr<sup>1,c</sup>

<sup>1</sup>AGH University of Science and Technology, Faculty of Metals Engineering and Industrial Computer Science, al. A. Mickiewicza 30, 30-059 Kraków, Poland

<sup>a\*</sup>sulek@agh.edu.pl, <sup>b</sup>matus@agh.edu.pl, <sup>c</sup>piotrkij00@gmail.com

**Keywords:** powder metallurgy; structural PM steels; analysis of variance (ANOVA).

### Abstract.

In the field of materials engineering, one of the main tasks is to design and manufacture a material with properties that allow it to be used in specific applications. The level of complexity and the amount of data coming from technological processes necessitate the applying advanced statistical techniques for their acquisition, processing and analysis.

The subject of the research was to evaluate the influence of production parameters, i.e.: chemical composition, sintering temperature, sintering atmosphere and heat treatment on tensile strength, bending strength and impact strength of four Fe-Mn-Cr-Mo-C steels produced by powder metallurgy (PM) technique. Sintering was carried out at temperatures of 1120 °C and 1250 °C in two types of protective atmospheres: 5% H<sub>2</sub>-95% N<sub>2</sub> and air + 52g of ferromanganese lumps (FeMn), then hardened [1].

Statistical analysis included the use of multivariate analysis of variance ANOVA (the so-called general linear model) and the planning of experiments DoE. The optimal ANOVA model was selected, taking into account only the main factors and interactions that significantly determine the behavior of the resulting parameter, without a significant reduction in the predictive power of the model. Taking into account the influence of the analyzed production parameters on all strength parameters, it can be concluded that the chemical composition, sintering temperature and the heat treatment performed have the greatest impact on the value of these properties. The sintering atmosphere has the smallest effect on the obtained properties.

The influence of the chemical composition may be caused by the different content of carbon and other alloying elements in steel (mainly chromium and molybdenum). At a lower carbon content (0.15% C), an increase both Cr and Mo content increases the tensile strength R<sub>m</sub>. However, the opposite effect is observed for bending strength and impact strength. At a higher carbon content (0.7% C), an increase the content of Mo and Cr causes a decrease in tensile and bending strength, while in the case of impact strength, its value increases. Increasing the sintering temperature, as well as carrying out additional heat treatment after the sintering process, increases the value of all of the analyzed properties.

The optimization of the manufacturing process and heat treatment of the tested materials was carried out for each analyzed strength parameter separately and for all strength parameters together. The aim of the optimization was to determine the setting of the sintering process parameter levels that would allow to obtain the maximum values of the analyzed mechanical properties.

### References

- [1] M. Sułowski, A. Jordan, A. Czarski, P. Matusiewicz, Estimation of the effect of production parameters on mechanical properties of sintered steels using ANOVA, Kraków, *Archives of Metallurgy and Materials* 62 (2017), 2, 571–576.

## Dynamic Fracture Characteristics of High-Strength Steel

Kianicová Marta<sup>1,b</sup>, Dlouhý Ivo<sup>2,c</sup>, Šandera Pavel<sup>3,d</sup>, Horníková Jana<sup>3,e</sup>  
and Pokluda Jaroslav<sup>1,3,a\*</sup>

<sup>1</sup>Faculty of Special Technology, Alexander Dubcek University of Trencin,  
Ku kyselke 469, 911 06 Trenčín, Slovakia

<sup>2</sup>Institute of Physics of Materials AS CR, Žižkova 22, 616 62 Brno, Czechia

<sup>3</sup>Faculty of Mechanical Engineering, Brno University of Technology,  
Technická 2, 616 69 Brno, Czechia

\*jaroslav.pokluda@tnuni.sk, <sup>b</sup>marta.kianicova@tnuni.sk, <sup>c</sup>idlouhy@ipm.cz,  
<sup>d</sup>sandera@fme.vutbr.cz, <sup>e</sup>hornikova@fme.vutbr.cz

**Keywords:** impact energy; fracture toughness; high strength steel; transition range.

### Abstract.

The absorbed impact energy and the dynamic fracture toughness  $K_{Id}$  of the low-alloyed steel OCHN3MFA were measured in respective temperature ranges  $\{-40, 90\}$  °C and  $\{-60, -20\}$  °C.

The values of absorbed impact energy were obtained in the range of  $\{14.1, 21.3\}$  J using Charpy V-notch samples fractured by the instrumented hammer Amsler (Zwick/Roell) after subtracting parasitic energies (friction in bearings, etc.). All these values corresponded to an extended transition region of the impact energy vs. temperature dependence. Indeed, the temperature  $-40$  °C was still higher than the lower impact-toughness threshold which confirmed the presence of distinct shear lips at the related fracture surfaces. Similarly, the temperature  $90$  °C was lower than the upper threshold since there was only 20 % of ductile morphology found at the related fracture surface. The dynamic fracture toughness was determined using the Charpy V-notch samples with fatigue pre-cracks fractured in the cryogenic chamber of the Zwick/Roell Z50 machine. Such obtained  $K_{Id}$ -values in the range of  $\{55.8, 77.5\}$  MPa·m<sup>1/2</sup> were found to be valid linear-elastic fracture toughness according to the standard [1]. Simultaneously, they were higher than the static  $K_{Ic}$  and  $K_{II}$  values reported in [2] for the corresponding temperature range.

This study revealed that the steel OCHN3MFA has a sufficient resistance to dynamic fracture which is particularly important with respect to special exploitation conditions of structural components made of this material.

### Acknowledgment

The research was funded by the Ministry of Education, Science, Research and Sport of the Slovak Republic, grant VEGA1/0346/19, and by the Brno University of Technology, specific research project FSI-S-20-6266.

### References

- [1] ASTM E399-20. Standard test method for linear-elastic plane-strain fracture toughness  $K_{Id}$  of metallic materials. In Annual Book of ASTM-Standards; ASTM International, Philadelphia, Pennsylvania, 2020.
- [2] J. Pokluda et al., Temperature Dependence of Fracture Characteristics of Various Heat-Treated Grades of Ultra-High-Strength Steel: Experimental and Modelling, *Materials* 14 (2021) 5875.

## Metallography of Fractured Aluminium Alloys for the Transmission System's Elements

Kreislova Katerina<sup>1,a\*</sup> and Turek Libor<sup>1,b</sup>

<sup>1</sup>SVUOM Ltd., U Mestanskeho pivovaru 934/4, 170 00 Prague 7, Czech Republic

<sup>a</sup>kreislova@svuom.cz, <sup>b</sup>turek@svuom.cz

**Keywords:** aluminium alloys; fractures; chemical composition; inhomogeneous structure; inclusions.

### Abstract.

An aluminium alloy is a composition consisting mainly of aluminium to which other elements have been added, e.g. include iron, copper, magnesium, silicon, and zinc. Their mechanical properties, manufacturability and service performance are the key issues during their application. Fractures have been reported on some elements from different aluminium alloys' construction elements from high voltage masts applied in Czech transmission system. The metallography was used for evaluation of fractured elements from different aluminium alloys' elements.

Although the fractured elements were casted from different aluminium alloys (superadutectic Al-Si, AlSi10Mg, Al0,7MgSi) the main reason of fractures was very similar for all of them – the low quality of casting, inhomogeneous structure and composition of matrix. Scanning electron microscopy (SEM), energy dispersive spectroscopy (EDAX) and conventional metallography were used to examine the effects of defects on fracture of cast parts. In evaluated aluminium structural elements, the two most prominent types of impurities are oxide films (alumina or spinel) and intermetallic particles – Fig. 1. The dominant component on the fracture surfaces is silicon, which forms clearly visible flat plates - sliding surfaces, and a high content of unwanted iron, which creates a brittle  $Al_5FeSi$  phase along the grain boundaries - it increases the tendency of the material to crack. The quartz concentration was ca twice into comparison with standards composition and reference matrix. The hard, intermetallic particles in aluminum alloys fracture before significant failure occur in the surrounding matrix [1]. The pores occurrences and incorporation of impurities in aluminium alloys can have a major effect on the properties of the material.

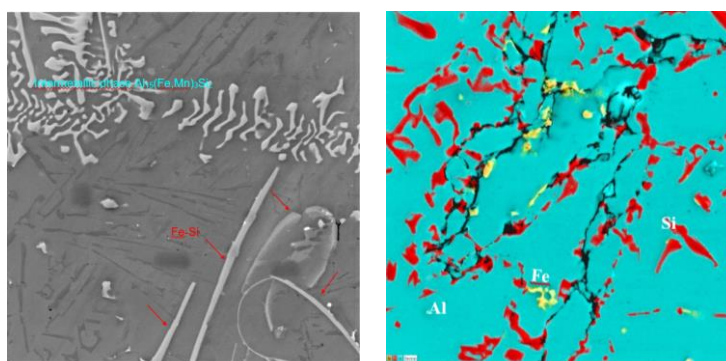


Fig. 1 SEM of structure of aluminium alloy's fracture surface.

### Acknowledgment

The study was performed and paper was written with support of project MPO - IP DKRVO, 2021.

### References

- [1] B. Wisner, A. Kontsos, In situ monitoring of particle fracture in aluminium alloys, *FFEMS* 41 (2018) 581-596.

## Fracture Mechanisms of Austenitic Steel Caused by Dynamic Tests

Uhríčik Milan<sup>1,a\*</sup>, Palček Peter<sup>1,b</sup>, Chalupová Mária<sup>1,c</sup>, Kuchariková Lenka<sup>1,d</sup>,  
Zatkalíková Viera<sup>1,e</sup>, Belan Juraj<sup>1,f</sup>, Oravcová Monika<sup>1,g</sup>  
and Pastierovičová Lucia<sup>1,h</sup>

<sup>1</sup>University of Žilina, Faculty of Mechanical Engineering, Department of Material Engineering,  
Univerzitná 8215/1, 010 26 Žilina, Slovakia

<sup>a\*</sup>milan.uhrick@fstroj.uniza.sk, <sup>b</sup>peter.palcek@fstroj.uniza.sk, <sup>c</sup>maria.chalupova@fstroj.uniza.sk,  
<sup>d</sup>lenka.kucharikova@fstroj.uniza.sk, <sup>e</sup>viera.zatkalikova@fstroj.uniza.sk, <sup>f</sup>juraj.belan@fstroj.uniza.sk,  
<sup>g</sup>monika.oravcova@fstroj.uniza.sk, <sup>h</sup>lucia.pastierovicova@fstroj.uniza.sk

**Keywords:** fracture; fatigue; austenitic steel; SEM; dynamic test.

### Abstract.

The article is focused on the analysis of fracture mechanisms of samples made of austenitic steel, which have been subjected to dynamic tests. Austenitic stainless steels are characterized as high corrosion resistant materials with high bio-tolerance and relatively high strength. They can be made strong by cold working and also can be made soft enough to be easily formed [1]. By cold working plastic deformation occurs. Austenitic steels are deformed by slipping and twinning during plastic deformation. The deformed region is presented by deformation twins and slip deformation [2]. Samples were used in two states, in the initial state and after chemical-thermal treatment. Dynamic tests to which samples were subjected were the impact test and the three-point bending test. Fracture areas were evaluated by scanning electron microscopy.

### Acknowledgment

The research was supported by the Scientific Grant Agency of the Ministry of Education of Slovak Republic and Slovak Academy of Sciences, VEGA 01/0134/20, and projects to support young researchers at UNIZA, the ID of projects 14877 and 12715.

### References

- [1] M.F. McGuire, *Stainless Steels for Design Engineers*, ASM International, Ohio, 2008.
- [2] R.E. Smallman, R.J. Bishop, *Modern Physical Metallurgy and Materials Engineering*, 6<sup>th</sup> ed., Reed Education and Professional Publishing Ltd, 1999.

## The Fractographic Analysis of Static and Fatigue Fracture Surfaces in Secondary A356 Aluminum Alloy With a Higher Concentration of Iron

Kuchariková Lenka<sup>1,a\*</sup>, Tillová Eva<sup>1,b</sup>, Chalupová Mária<sup>1,c</sup>, Uhrčík Milan<sup>1,d</sup>, Pastierovičová Lucia<sup>1,e</sup> and Belan Juraj<sup>1,f</sup>

<sup>1</sup>University of Žilina, Faculty of Mechanical Engineering, Department of Materials Engineering, Univerzitná 8215/1, 010 26 Žilina, Slovakia

<sup>a\*</sup>lenka.kucharikova@fstroj.uniza.sk, <sup>b</sup>eva.tilova@fstroj.uniza.sk,

<sup>c</sup>maria.chalupova@fstroj.uniza.sk, <sup>d</sup>milan.uhricik@fstroj.uniza.sk,

<sup>e</sup>lucia.pastierovicova@fstroj.uniza.sk, <sup>f</sup>juraj.belan@fstroj.uniza.sk

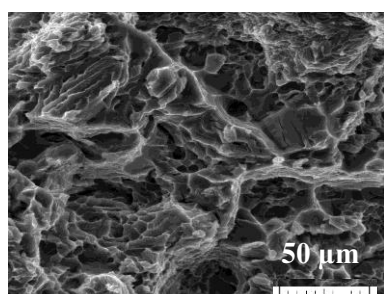
**Keywords:** fractography; secondary Al alloys; Fe impurity; fracture surfaces, fracture of Fe-rich phases.

### Abstract.

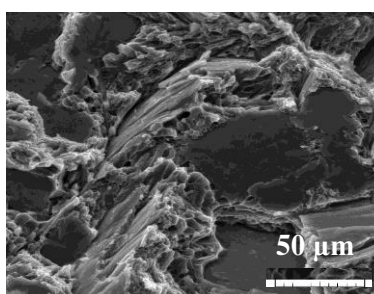
Metal scrap and waste may be used for producing high-quality alloys, but a significant number of different metals are present in aluminum alloy scrap and waste. Iron is a common impurity and element, which prevents the casting from sticking to the mold. The Fe reduction is a very economically and technologically expensive process and therefore there is a growing interest in researching such materials. Increasing content of Fe lead to the formation of a higher amount of Fe-rich plate-like phases. The plate-like phases lead to the formation of cleavage fracture in fracture surfaces. Therefore, materials with higher content of Fe are interesting for research. Based on these facts, this study aims to analyze the effect of higher Fe content (Table 1) on fracture surfaces in A356 cast alloys. This study confirms the increasing amount of Fe-rich phases in the plate-like form in the melt with higher content of Fe. The increasing amount leads to the formation of large cleavage fractures on fracture surfaces (Fig. 1). Although the cleavage fracture increased, the experimental results show low changes in the properties of all experimental melts.

Table 1 Chemical composition of experimental materials [wt. %]

Melt	Al	Si	Mg	Fe	Cu	Mn	Ti	Sn	Sb	Other
A	92.253	7.028	0.354	<b>0.123</b>	0.013	0.009	0.123	0.004	0.007	remainder
B	91.673	7.340	0.302	<b>0.454</b>	0.021	0.009	0.118	0.006	-	remainder
C	91.486	7.315	0.292	<b>0.655</b>	0.03	0.01	0.12	0.005	-	remainder



a)



b)

Fig. 1 Effect of higher Fe content on the fracture surface in A356 cast alloy, SEM. a), melt A – 0.123 % of Fe; b), melt C – 0.655 % of Fe.

### Acknowledgment

The research was supported by the Scientific Grant Agency of the Ministry of Education of Slovak Republic and Slovak Academy of Sciences, VEGA 01/0398/19, KEGA 016ŽU-4/2020, and project to support young researchers at UNIZA, the ID of project 12715-project leader Ing. Lenka Kuchariková.

## Microstructure Characterization of Fe-Based Nanomaterials by High-Energy X-ray Scattering Techniques

Baldovský Andrej<sup>1,a\*</sup>, Yudina Daria<sup>1,b</sup>, Girman Vladimír<sup>1,c</sup>,  
Lisnichuk Maksym<sup>1,d</sup>, Sovák Pavol<sup>1,e</sup> and Bednarčík Jozef<sup>1,2,f</sup>

<sup>1</sup>Institute of Physics, Faculty of Science, P. J. Šafárik University in Košice,  
Park Angelinum 9, 041 54 Košice, Slovakia;

<sup>2</sup>Institute of Experimental Physics, Slovak Academy of Sciences,  
Watsonova 47, 040 01 Košice, Slovakia;

<sup>a\*</sup>andrej.baldovsky@student.upjs.sk, <sup>b</sup>daria.yudina@student.upjs.sk, <sup>c</sup>vladimir.girman@upjs.sk;  
<sup>d</sup>maksym.lisnichuk@upjs.sk, <sup>e</sup>pavol.sovak@upjs.sk; <sup>f</sup>jozef.bednarcik@upjs.sk

**Keywords:** nanocrystalline; microstructure; grain size; X-ray diffraction.

### Abstract.

Fe-based nanomaterials are known for their excellent soft magnetic properties such as low coercivity, high saturation magnetization, high permeability and low power losses. Their unique properties are due to characteristic microstructure consisting of nanosized crystals homogeneously dispersed within a major amorphous phase. High-energy X-ray scattering of synchrotron radiation is a powerful method to qualitatively and quantitatively describe atomic structure of highly disordered materials such as nanocrystalline and amorphous alloys. Main aim of this work is to quantitatively describe microstructure (mean grain size of nanocrystals) of Fe-based alloy using reciprocal (Scherrer equation) and real space (pair distribution function - PDF) techniques. X-ray scattering experiments were performed at the P02.1 beamline of the electron storage ring PETRA III at DESY (Hamburg, DE). Special emphasis was placed on resolving impact of instrument angular resolution on grain size determined by reciprocal and real space techniques. Sample to detector distance was systematically changed to improve angular resolution of the instrument and thus precisely determine grain size.

### Acknowledgment

The authors are grateful for the financial support received from the project VEGA 1/0406/20. We acknowledge DESY (Hamburg, Germany), a member of the Helmholtz Association HGF, for the provision of experimental facilities.

## Thermal Shock Resistance of Ultra High Temperature ZrB<sub>2</sub> Ceramic Composites

Ivor Michal<sup>1,2a\*</sup>, Kovalčíková Alexandra<sup>2</sup> and Dusza Ján<sup>2</sup>

<sup>1</sup>Technical University of Košice, Faculty of Materials, Metallurgy and Recycling, Institute of Materials and Quality Engineering, Letná 9, 042 00 Košice, Slovakia

<sup>2</sup>Institute of Materials Research, Slovak Academy of Sciences, Watsonova 47, 040 01 Košice, Slovakia

<sup>a</sup>mivor@saske.sk

**Keywords:** UHTC materials; ZrB<sub>2</sub> composites; thermal shock resistance.

### Abstract.

The recent investigation of ceramic materials discovered high sensitivity to thermal shock. Temperature changes caused by inhomogeneous temperature distribution are responsible for extension of existing cracks in the structure of ceramics. Appropriate material selection and design of components lead to minimize of thermal stresses.

ZrB<sub>2</sub> ceramic matrix composites were considered in our analysis. The effect of three different additives (ZrC, B<sub>4</sub>C, and SiC) on thermal shock stability of ZrB<sub>2</sub> was measured by indentation quenching method. The indented samples were inserted to laboratory furnace and heated to precisely defined temperature at air atmosphere. Dwell temperature was 20 min and then the samples were quenched in water at room temperature. After this procedure the crack lengths were measured with an optical microscope. The measurement was repeated at increasing quench temperature  $\Delta T$  until the critical temperature  $\Delta T_c$  was reached and radial crack became unstable.

The effect of additives on thermal shock resistance of prepared composites was different and it is also reflected in the critical temperature of crack growth propagation. The highest thermal shock resistance showed ZrB<sub>2</sub> + 10% SiC composite. The critical temperature of ZrB<sub>2</sub> + 10% SiC was around 550°C and critical temperatures of ZrB<sub>2</sub> + 10% B<sub>4</sub>C and ZrB<sub>2</sub> + 10% ZrC were 300°C and 350°C, respectively.

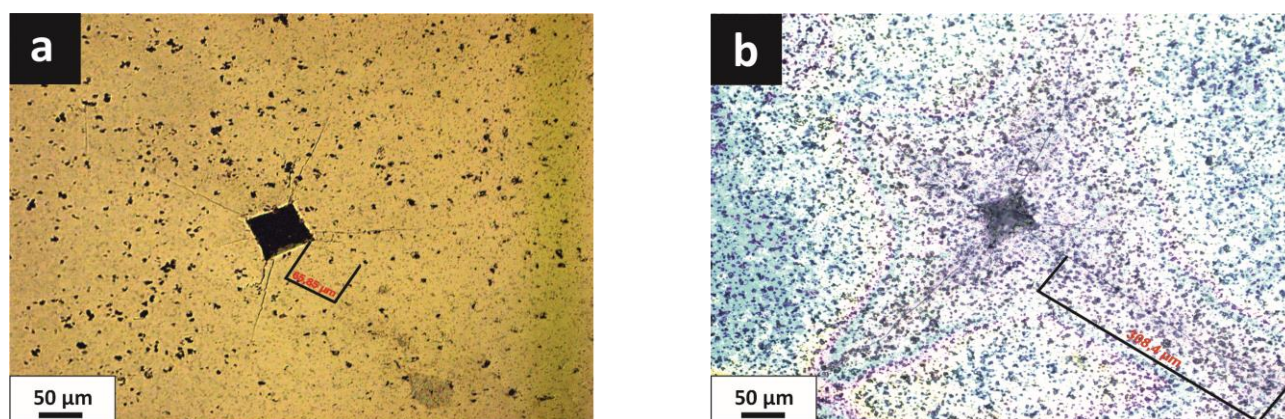


Fig. 1 Cracks formation in a ZrB<sub>2</sub> + 10wt.% B<sub>4</sub>C; a) sample cracks growth at room temperature, b) unstable cracks growth after quenching at 350°C.

### Acknowledgment

The research was supported by the Grant Agency of the Slovak Academy of Sciences through project APVV-17-0328, VEGA -2/0118/20, VEGA -2/0137/22.

## Ceramic Nano/Microfibers as Filler for Composites

Koribanich Ihor<sup>1,2,a\*</sup>, Mudra Erika<sup>1</sup>, Kovalcikova Alexandra<sup>1</sup>, Shepa Ivan<sup>1</sup>,  
Girman Vladimir<sup>3</sup>, Hrubovcakova Monika<sup>1</sup>, Pavlinak David<sup>4</sup>, Balaz Matej<sup>5</sup>,  
and Dusza Jan<sup>1</sup>

<sup>1</sup>Institute of Materials Research, Slovak Academy of Sciences,  
Watsonova 47, 040 01, Kosice, Slovak Republic

<sup>2</sup>Faculty of Materials, Metallurgy and Recycling, Technical University of Kosice,  
Letna 9, 040 01, Kosice, Slovak Republic

<sup>3</sup>Institute of Physics, Faculty of Science P.J. Safarik University,  
Park Angelinum 9, 040 01, Kosice, Slovak Republic

<sup>4</sup>Department of Physical Electronics, Masaryk University, Kotlarska 2, 61137 Brno, Czechia

<sup>5</sup>Institute of Geotechnics, Slovak Academy of Sciences,  
Watsonova 45, 040 01 Kosice, Slovak Republic

\*a:ikoribanich@saske.sk

**Keywords:** alumina; fibers; graphene; electrospinning.

### Abstract.

The present work is focused on preparation and characterization of composite nano/microfibers based on alumina. These Al<sub>2</sub>O<sub>3</sub> fibers are coated with a thin layer of graphene oxide (GO) and are applicable as fillers in composites. The preparation of Al<sub>2</sub>O<sub>3</sub>/GO fibers is carried out in the following steps: preparation of the solution and produce of polymer fibers by electrospinning (ES), calcination of precursor fibers at 1100 and 1200 °C and coating a thin graphene-based layer to the fibers by Chemical Vapor Deposition (CVD) method. The phase composition and morphology of the composite fibers were characterized by X-ray diffraction (XRD), X-ray Photoelectron Spectroscopy (XPS) analysis, Raman spectroscopy, scanning and transmission electron (SEM and TEM) microscopy. The porosity of the final fibers was evaluated by Bruanuer-Emmet-Teller (BET) analysis.

The surface of composite fibers were smooth and their diameters was about 200-600 nm. The mechanism of phase transformation at 1100 °C led to formation of the mixture of  $\gamma$ -Al<sub>2</sub>O<sub>3</sub> and  $\alpha$ -Al<sub>2</sub>O<sub>3</sub>. Increasing the temperature of heat treatment up to 1200 °C resulted in the formation of pure  $\alpha$ -Al<sub>2</sub>O<sub>3</sub> phase. TEM results confirmed that the alumina fibers are covered by 3–4 layers of graphene - based structure. The specific surface area of pure alumina fibers after graphene oxide application slightly decreased from 34 m<sup>2</sup>/g to 27 m<sup>2</sup>/g, which means that carbon probably got into the pores present. Raman spectroscopy and XPS analysis were evaluated, that the surface layer of fibers is formed as graphene oxide (GO). The presence of GO layer on Al<sub>2</sub>O<sub>3</sub>/GO fibers results in increasing electrical conductivity and wear protection of the potential composites.

### Acknowledgment

This work was realized within the frame of the project VEGA-2/0137/22 and APVV-17-0625.

## Microstructural Analysis of EuBCO Bulks With and Without Holes

Kuchárová Veronika<sup>1,a\*</sup>, Diko Pavel<sup>1,b</sup>, Lojka Michal<sup>2,3,c</sup>, Hlásek Tomáš<sup>2,d</sup>  
and Plecháček Vladimír<sup>2,e</sup>

<sup>1</sup>Institute of Experimental Physics, Slovak Academy of Sciences, Watsonova 47, Kosice, Slovakia

<sup>2</sup>CAN Superconductors, Ringhofferova 66, Kamenice, Czech Republic

<sup>3</sup>Faculty of Chemical Technology, University of Chemistry and Technology, Technická 5, Prague 6, Czech Republic

<sup>a\*</sup>kucharova@saske.sk, <sup>b</sup>dikos@saske.sk, <sup>c</sup>michal.lojka@can-superconductors.com,  
<sup>d</sup>tomas.hlasek@can-superconductors.com, <sup>e</sup>vladimir.plechacek@can-superconductors.com

**Keywords:** EuBCO bulk superconductor with artificial holes; microstructure.

### Abstract.

Several techniques have been proposed to enhance the macroscopic superconducting properties of REBCO bulk singlegrain superconductors (BSS). One possibility is to drill holes in the BSS, which should both reduce the porosity of the BSS by allowing gases to escape from the molten sample, but also facilitate the oxygenation of the crystals during the conversion of the tetragonal phase RE123 to the orthorhombic superconducting phase.

In this work we present the results of microstructural analyses of EuBCO-Ag BSS with and without holes grown using a top-seed melt-growth process. The microstructure was analysed by polarized light microscopy, scanning electron microscopy and image processing. It has been shown that holes cause lower porosity of the *a*-growth sectors and lower density of *a/c*-oxidation cracks in the non-porous areas along the holes (Fig. 1). Other microstructural features such as higher volume fraction of Eu<sub>2</sub>BaCuO<sub>5</sub> particles in the *a*-growth sector than in the *c*-growth sector, even distribution of Ag particles in the samples, presence of tetragonal areas of EuBa<sub>2</sub>Cu<sub>3</sub>O<sub>7-x</sub> also appear to be similar on both types of samples and cannot significantly affect macroscopic superconducting properties.

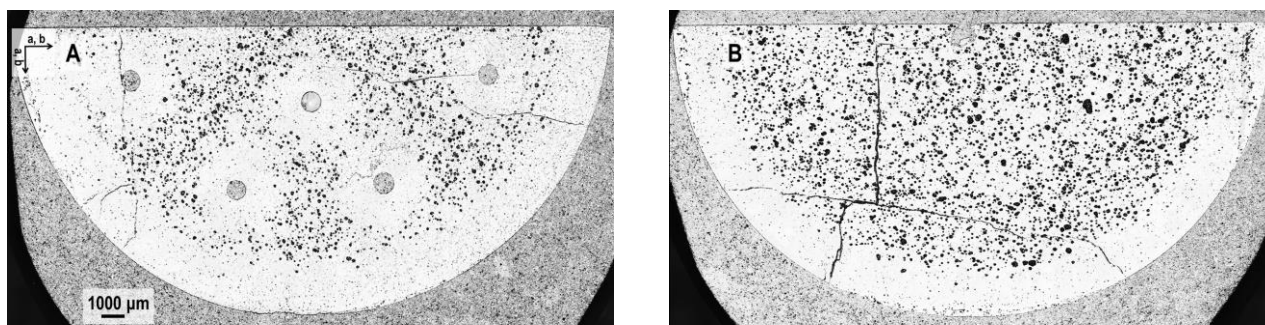


Fig. 1 Polished a/b surface of the sample with holes (A) and sample without holes (B) at the half of the sample height

### Acknowledgment

This work was supported by APVV-17-0625 and VEGA No. 2/0094/22 projects.

## Influence of Ligands on Physicochemical Characteristics of Magnetic Nanoparticles

Szucsova Jaroslava<sup>1,a\*</sup>, Zelenakova Adriana<sup>1,b</sup>, Nagy Lubos<sup>1</sup>, Barutiak Michael<sup>1</sup>, Benova Eva<sup>2</sup>, Zelenak Vladimir<sup>2</sup> and Zavisova Vlasta<sup>3</sup>

<sup>1</sup>Department of Condensed Matter Physics, Pavol Jozef Safarik University in Kosice, Park Angelinum 9, 040 01 Kosice, Slovakia

<sup>2</sup>Department of Inorganic Chemistry, Pavol Jozef Safarik University in Kosice, Moyzesova 11, 040 01 Kosice, Slovakia

<sup>3</sup>Institute of Experimental Physics, Watsonova 47, 040 01 Kosice, Slovakia

<sup>a\*</sup>jaroslava.szucsova@upjs.sk, <sup>b</sup>adriana.zelenakova@upjs.sk

**Keywords:** magnetic nanoparticles; ligand; SEM; core-shell; biomedical applications.

### Abstract.

Magnetic nanoparticles are widely applied in many technological fields and in recent years also the specialists in medicine are trying to utilize their unique and scalable properties such as high surface-to-volume ratio, high mobility in free state and their ability to enter cells or be designed to bind to specific cells. Recent pandemic shows that conventional magnetic nanoparticles with modified surface can be used for effective magnetic separation of DNA and RNA samples and also in diagnostic of different range of viruses.

In presented work we prepared and characterized core-shell magnetic nanoparticle samples consisted of Fe<sub>3</sub>O<sub>4</sub> core coated with SiO<sub>2</sub> shell. Samples were coated with ligands APTES ((3-Aminopropyl)triethoxysilane), CPTMS ((3-Chloropropyl)trimethoxysilane) and MMSP (Monomethyl-sulfonyl-peroxide). Such samples were further investigated for their magnetic properties, size and morphology. Magnetic properties were studied in DC field up to 5 T in temperature range 2-300 K. Size and morphology were determined from SEM micrographs and elemental compositions of the samples were investigated using EDX analysis.

Modification of nanoparticle surface with different ligands leads to modification of active centers on the SiO<sub>2</sub> surface on which the DNA and RNA molecules can be bounded. It also causes the change in magnetic and structural properties of nanoparticles.

### Acknowledgment

This work was supported by the Development Operational Programme Integrated Infrastructure for the project “Nanoparticles for solving diagnostic-therapeutic problems with COVID-19 (NANOVIR)”, ITMS 2014 +:313011AUW7, co-founded by the European Regional Development Fund (ERDF) and by the Slovak Research and the Development Agency under the contract No. APVV-20-0512.

## Processing and Mechanical Properties of (Hf-Ta-Zr-Nb-Ti)C

Timkova Lenka<sup>1,2a\*</sup>, Csanadi Tamas<sup>1</sup>, Hrubovcakova Monika<sup>2</sup>, Kovalcikova Alexandra<sup>2</sup>, Naughton Duszova Annamaria<sup>2</sup>, Vaskova Iveta<sup>1</sup> and Dusza Jan<sup>2</sup>

<sup>1</sup>Technical University of Kosice, Faculty of Materials, Metallurgy and Recycling, Institute of Materials, Letna 9, 042 00 Kosice, Slovakia

<sup>2</sup>Institute of Materials Research, Slovak Academy of Science, Watsonova 47, 040 01 Kosice, Slovakia

\*altimkova@saske.sk

**Keywords:** high-entropy carbide; spark plasma sintering; nanoindentation.

### Abstract.

Recently, single-phase solid solutions (SS) containing multiple transition metal carbides called high-entropy carbide (HEC) ceramics have attracted interest due to their higher hardness and elastic modulus compared to the individual carbides. The aim of the present contribution is to study the influence of the processing route on the hardness and indentation Young's modulus of the high-entropy (Hf-Ta-Zr-Nb-Ti)C carbide. The experimental materials were prepared by ball milling and spark plasma sintering (SPS) method on the temperature 2100°C. The effect of sintering time (5 min, 10 min and 20 min) on the microstructure development and properties of investigated systems has been investigated. The microstructure analysis performed using scanning electron microscopy (SEM) on the polished surface. The measured grain size values were from 5 µm to 14 µm. Nano indentation was performed using Nano-indenter Agilent G200. The measured values of indentation hardness were from 36 GPa to 39 GPa and indentation modulus of elasticity were from 558 GPa to 577 GPa, respectively. Vickers hardness was performed using Wolpert Wilson 432 SVD Vickers Hardness tester. An indentation method using a Vickers indenter was used to determine the indentation fracture resistance - fracture toughness. Loads from 1 – 5 kg with a loading time of 10 s at room temperature were used. The measured values of indentation fracture resistance were from 2.70 MPa to 3.50 MPa, respectively.

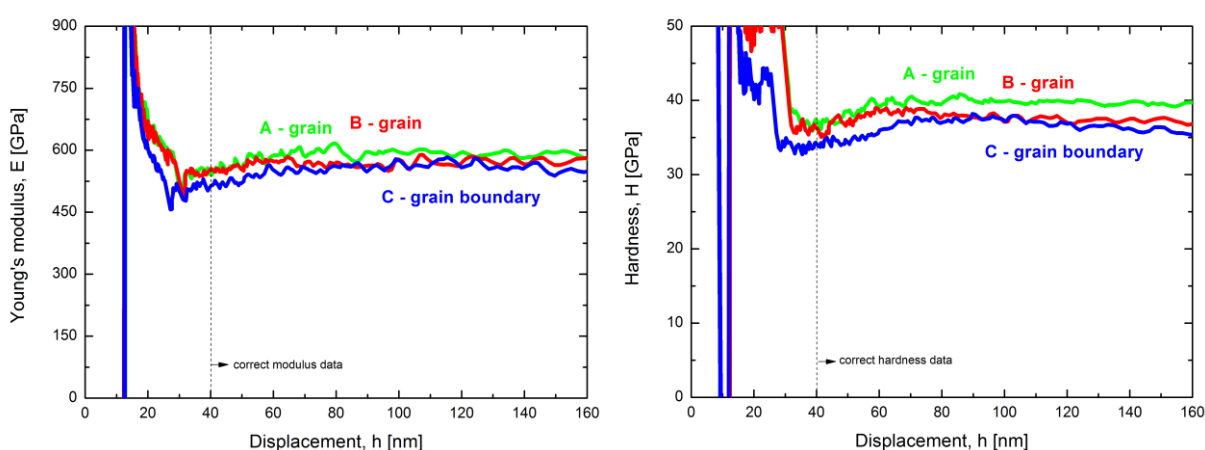


Fig. 1 The characteristic value of (Hf-Ta-Zr-Nb-Ti)C system: hardness and Young's modulus displacement profiles of locations inside the grains (A, B), and at a grain boundary (C).

### Acknowledgment

The research was supported by the Grant Agency of the Slovak Academy of Sciences through project VEGA No. 2/0118/20 and APVV-19-0497.

## Microstructure of YBCO Bulk Samples Grown via 45°-Twin-Seeds

Zmorayova Katarina<sup>1,a\*</sup>, Diko Pavel<sup>1</sup> and Yao Xin<sup>2</sup>

<sup>1</sup>Institute of Experimental Physics, Slovak Academy of Sciences,  
Watsonova 47, 04001, Kosice, Slovakia

<sup>2</sup>Shanghai Jiao Tong Univ, Sch Phys & Astron, Key Lab Artificial Struct & Quantum Control, State  
Key Lab Met Matrix Composites, Minist Educ, Dongchuan Rd 800, Shanghai 200240,  
Peoples R China

\*[azmoray@saske.sk](mailto:azmoray@saske.sk)

**Keywords:** YBCO bulk samples; microstructure; crystal growth; subgrain structure; crystal contact boundary, growth sectors boundary.

### Abstract.

In this work, the microstructural behavior of YBCO bulk samples grown via 45°-twin-seeds is presented. The microstructure was studied by polarized light microscopy and scanning electron microscopy. It turns out that crystal growth can be well described by visualizing the structure of subgrains. Dominant are the subgrains oriented longitudinally in the growth direction of the growing tetragonal  $\text{YBa}_2\text{Cu}_3\text{O}_x$  (Y123) crystal (so-called a-subgrains), which are perpendicular to the growth front of the Y123 crystal. Analysis of the subgrain structure shows that only growth in the  $\langle 100 \rangle$  direction was active during Y123 bulk crystal growth. Visualization of the subgrain structure allowed us to determine the contact boundary between two growing Y123 crystals (crystal contact boundary: CCB), as well as the boundary between the a-growth sectors (a/a-GSB). While for greater seed spacing, a/a-GSB is straight as for the Y123 crystal growing from one seed, for shorter seed spacing, a/a-GSB bends and two a/a-GSBs meet within Y123 bulk. The conditions of the observed behavior will be discussed in the contribution.

## Development and Research of Copper Filter for Full Face Masks Prepared by Powder Metallurgy Technology

Ballóková Beáta<sup>1,a\*</sup>, Molčanová Zuzana<sup>1,b</sup>, Brestovič Tomáš<sup>2,c</sup>,  
Jasminská Natália<sup>2,d</sup>, Michalik Štefan<sup>3,e</sup> and Saksli Karel<sup>1,f</sup>

<sup>1</sup>Institute of Materials Research SAS, Watsonova 47, Košice, Slovakia

<sup>2</sup>Faculty of Mechanical Engineering, Technical University of Košice,  
Letná 9, 042 00 Košice, Slovak Republic

<sup>3</sup>Diamond Light Source Ltd., Harwell Science and Innovation Campus,  
Didcot, Oxfordshire OX11 0DE, UK

<sup>a\*</sup>bbalokova@saske.sk, <sup>b</sup>molcanova@saske.sk, <sup>c</sup>tomas.brestovic@tuke.sk,  
<sup>d</sup>natalia.jasminska@tuke.sk, <sup>e</sup>stefan.michalik@diamond.ac.uk, <sup>f</sup>ksaksl@saske.sk

**Keywords:** powder technology; copper filter; pressure losses; X-ray tomography.

### Abstract.

Copper in different formats has been used in research and clinical settings to reduce the risk of bacterial and viral contamination. Copper can eliminate pathogenic organisms after a short period of exposure. Despite significant reduction on infectivity of SARS-1,2 after 3 h in aerosols, 72 h on plastic, and 48 h on stainless steel, the virus remained infectious. After exposition on copper, no viable virus was observed after 8 h and after 4 h for SARS-CoV-1,2.

In this paper we present results of development and research of copper filter produced by powder technology. Technological parameters, microstructure, EDX analysis, fractography Cu filters are reported. Measurements of pressure losses of the filters for a dynamic air viscosity of  $1.82 \cdot 10^{-5}$  Pa.s and an air density of  $1.167 \text{ kg/m}^3$  were performed. The pressure losses of the P-Cu-AW315 filter show a very favorable value for use in full face masks and there are in accordance with the standard EN 149, Fig.1. The X-ray tomography measurement was carried out at the I12-JEEP beamline. The reconstructed 3D images were visualized and analyzed by Avizo Lite 2020.2 software. The relative volume of grains and pores was estimated (on the base of segmentation results) to be roughly about 50% to 50% in the investigated specimen volume. Figure 2 shows a reconstructed 3D image of the specimen together with selected xz projections after performing segmentation based on thresholding settings.

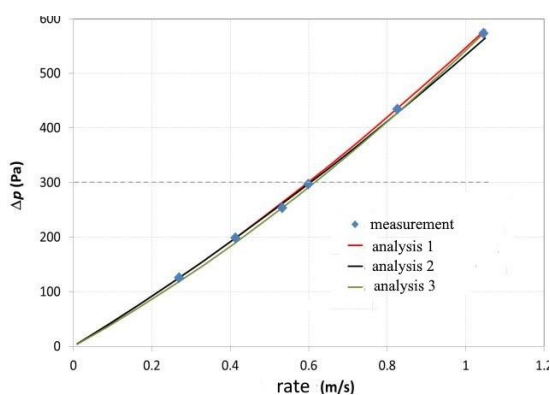


Fig.1 Dependence of pressure loss on air flow rate.

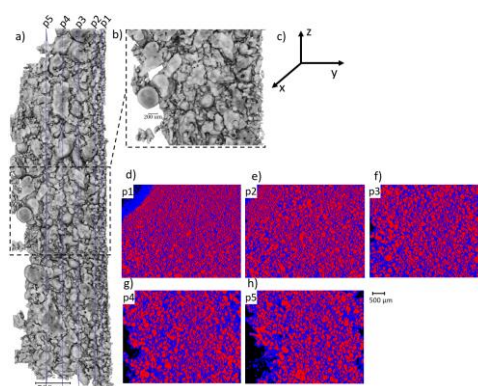


Fig.2 A reconstructed 3D image of the specimen together with selected xz projections.

### Acknowledgment

This work was supported by the agencies: PP-APVV-20-0025 and VEGA 2/0039/22.

## Formation of Alpha-Case Layer During Oxidation of Ti6Al4V Surface by Annealing at 1050 °C and Change of Microstructure After Different Cooling Rates

Belan Juraj<sup>1,a\*</sup>, Uhrčík Milan<sup>1,b</sup>, Kucháriková Lenka<sup>1,c</sup>, Tillová Eva<sup>1,d</sup>  
and Pastierovičová Lucia<sup>1,e</sup>

<sup>1</sup>Department of Materials Engineering, Faculty of Mechanical Engineering, University of Žilina, Univerzitná 8215/1, 01026 Žilina, Slovakia

<sup>a\*</sup>juraj.belan@fstroj.uniza.sk, <sup>b</sup>milan.uhrick@fstroj.uniza.sk, <sup>c</sup>lenka.kucharikova@fstroj.uniza.sk, <sup>d</sup>eva.tilova@fstroj.uniza.sk, <sup>e</sup>lucia.pastierovicova@fstroj.uniza.sk

**Keywords:** alpha-case layer; oxidation; Ti6Al4V alloy; annealing; microstructure changes.

### Abstract.

The two-phase titanium alloy Ti6Al4V (often referred to as GRADE 5 or Ti64) is currently probably the most widely used type of Ti alloy. It is characterized by an excellent combination of strength - toughness - chemical stability. However, at temperatures above 500°C - 800°C it is prone to the diffusion of oxygen into surface layers, where the increased oxygen content creates the so-called "alpha-case" layer. The formation of this layer is associated with a reduction mainly in the deformation characteristics of the alloy. The paper focuses on the metallographic analysis of the "alpha-case" layer after annealing at 1050°C with a holding time of 3 hours and cooled at different cooling rates (500°C/s, 1°C/s and 0.08°C/s), see Figure 1. Microstructure changes were observed by light microscopy using polarized light - PL, dark field - DF and phases were identified by SEM methods. The influence of changes in the microstructure on the mechanical properties was determined by measuring the microhardness HV0.2 / 10 (STN EN ISO 6507) with Zwick / Roell ZHμ and measuring the resistance to impact stress KU (Charpy system STN EN 10045-1). Based on the microhardness measurement, an increase in the microhardness of the surface layers was observed at all cooling rates and at the same time a decrease in the impact resistance was observed compared to the initial state.

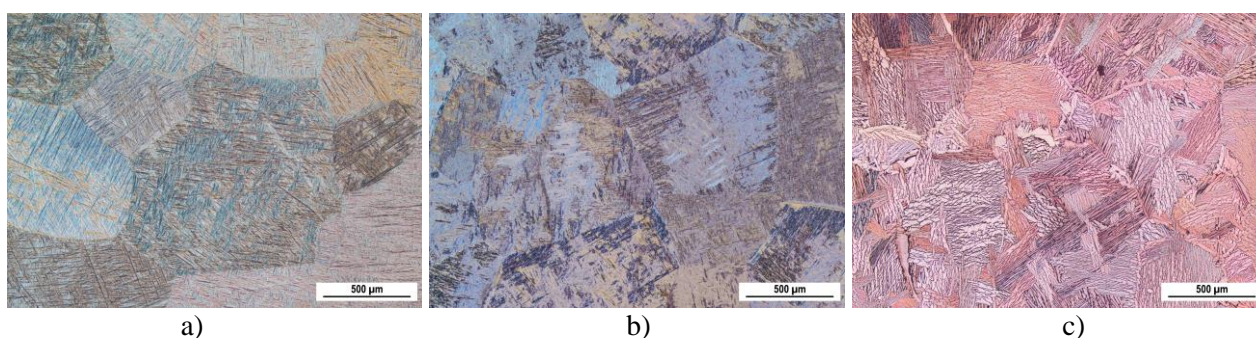


Fig. 1 Microstructures representing various cooling rates of Ti6Al4V alloy after applied annealing above  $\beta$ -transus at temperature 1050°C with 3 hours dwell, a) water cooling 500°C/s, b) air cooling 1°C/s, and c) furnace cooling 0.08°C/s; etched by 1.5ml HF + 2ml HNO<sub>3</sub> + 10ml H<sub>2</sub>O, PL observation.

### Acknowledgement

The authors acknowledge the KEGA project 016ŽU-4/2020 and the VEGA project 01/0398/19 for the financial support of this work.

## Direct Production of Tin Bronzes from Copper and Cassiterite

Haubner Roland<sup>1,a\*</sup> and Strobl Susanne<sup>1,b</sup>

<sup>1</sup>Technische Universität Wien, Institute of Chemical Technologies and Analytics,  
Getreidemarkt 9/164-03, A-1060 Vienna, Austria

<sup>a\*</sup>roland.haubner@tuwien.ac.at, <sup>b</sup>susanne.strobl@tuwien.ac.at

**Keywords:** bronze; cassiterite; archaeometallurgy.

### Abstract.

In the Bronze Age several possibilities for tin bronzes production were available, namely direct from copper and cassiterite ore ( $\text{SnO}_2$ ) or by alloying copper with metallic tin. Experiments were performed to verify the method of direct bronze production by adding cassiterite to molten copper.

Cassiterite ores from Cornwall and Schlaggenwald were available. In self-made clay crucibles copper was covered with charcoal and melted at 1090 °C. 10 wt. % cassiterite ore (Fig. 1b) was added to the copper melt and again covered with charcoal. Approximately after 15 minutes the furnace was switched off and the melt was cooled slowly.

The samples were prepared by metallographic methods and examined by LOM and SEM. Depending on the ores between 4 and 7 wt.% Sn were measured in the bronze alloys. The microstructures of the bronzes are dendritic, with copper enriched dendrites and Sn enrichment in the interdendritic areas.

It can be confirmed by these experiments that the direct production of tin bronzes from copper and cassiterite ore is possible.

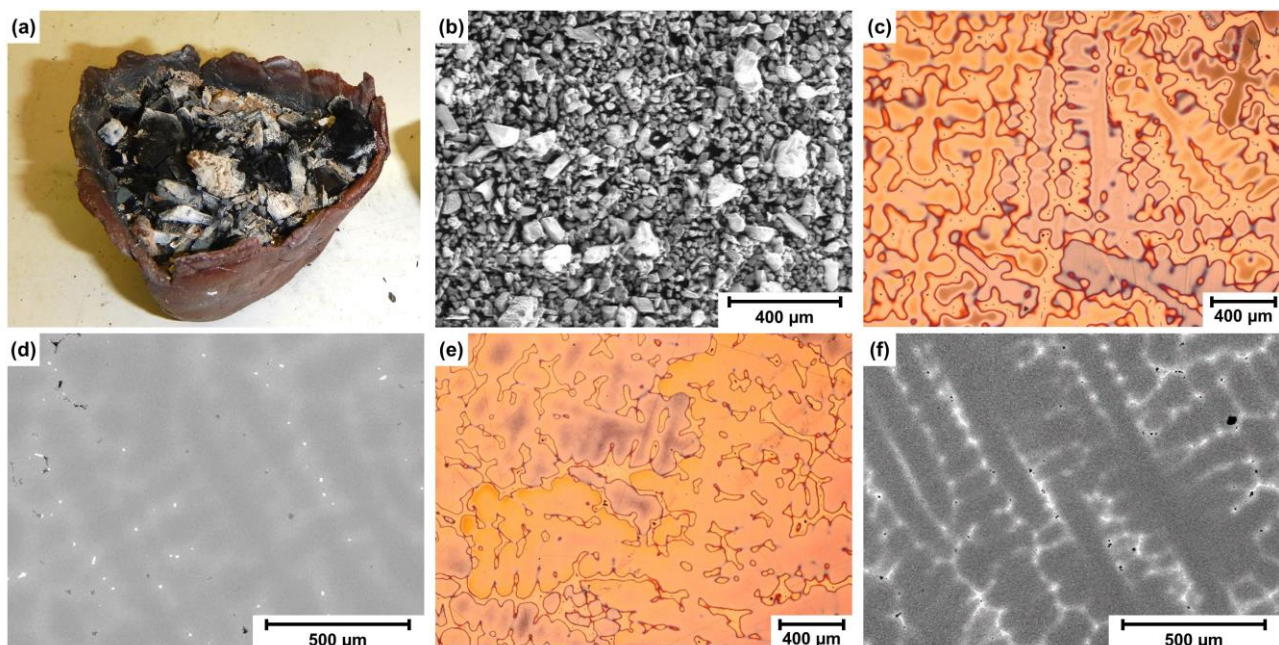


Fig. 1 (a) Clay crucible after the experiment, (b) Cassiterite ore from Cornwall, (c – f) dendritic microstructures of the produced tin bronzes, (c, e) LOM, (d, f) SEM.

## Influence of Cavitation in Seawater on the Etching Attack of Manganese-Aluminum-Bronzes (MAB)

Linhardt Paul<sup>1,a</sup>, Biezma Maria Victoria<sup>2,b</sup>, Strobl Susanne<sup>1,c</sup> and Haubner Roland<sup>1,d\*</sup>

<sup>1</sup>Technische Universität Wien, Institute of Chemical Technologies and Analytics, Getreidemarkt 9/164-03, A-1060 Vienna, Austria

<sup>2</sup>University of Cantabria, Dique de Gamazo, 1 Santander, Spain

<sup>a</sup>paul.linhardt@tuwien.ac.at, <sup>b</sup>biezmav@unican.es, <sup>c</sup>susanne.strobl@tuwien.ac.at, <sup>d\*</sup>roland.haubner@tuwien.ac.at

**Keywords:** manganese-aluminum-bronze; cavitation; etching; seawater.

### Abstract.

During cavitation investigations with manganese-aluminum-bronzes (MAB) in seawater, it was found that the microstructure of the bronze was developed by etching [1]. To investigate this phenomenon in more detail, metallographically polished MAB samples were treated with pulsed ultrasound in a beaker with synthetic seawater (Fig. 1a).

Fig. 1b shows a sample after 3 minutes of ultrasonic treatment in seawater and Fig. 1d after 5 minutes. The stronger etching after 5 min attack can be seen clearly. It is striking that a halo forms around the kappa phase, which can reach a diameter of up to 200  $\mu\text{m}$ .

SEM images (Fig.1c, f) show that the kappa phase is more strongly attacked. This could be due to preferential local steam bubble formation and cavitation, where the kappa phase is dissolved or breaks out.

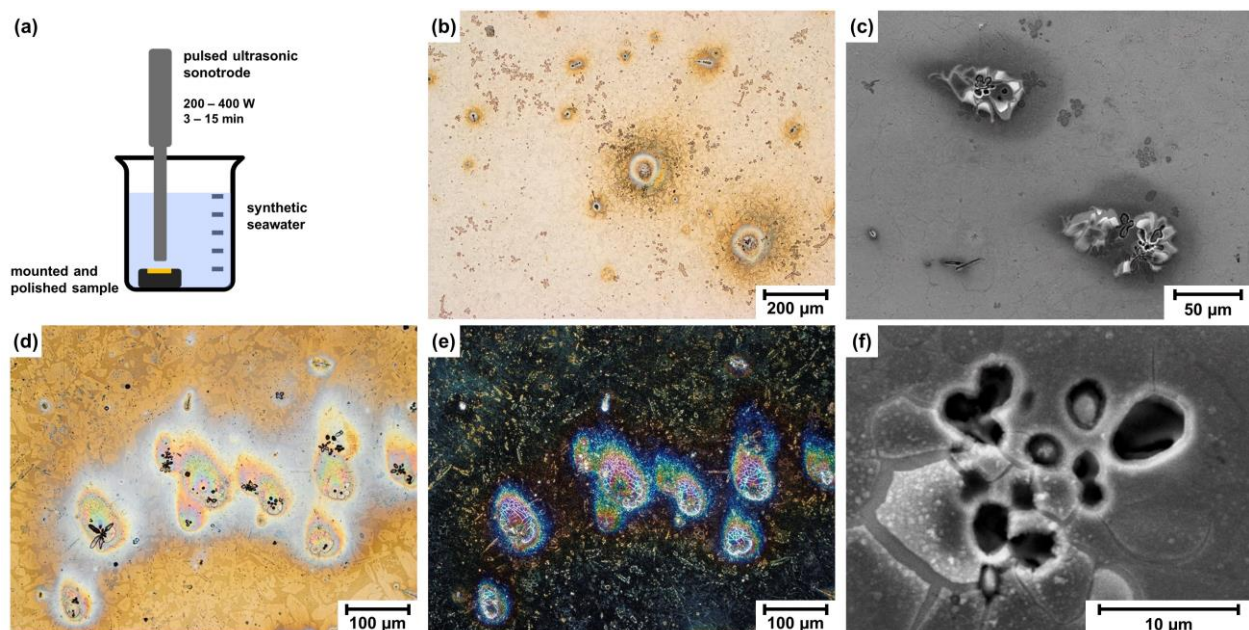


Fig. 1 MAB surfaces after an ultrasound treatment, (a) Scheme of the experimental setup (b) 3 min. treatment. (c, f) SEM pictures, (d, e) 5 min treatment, (e) polarized light.

### References

- [1] N.M. Mota, S.S.M. Tavares, A. Nascimento, G. Zeeman, M.V. Biezma Moraleda, Failure analysis of a butterfly valve made with Nickel Aluminum Bronze (NAB) and Manganese Aluminum Bronze (MAB), *Engineering Failure Analysis*, 129 (2021) 105732.

## The Yttrium Substitution Impact on the Mechanical Properties of Biodegradable Mg<sub>66</sub>Zn<sub>30</sub>Ca<sub>4</sub> Alloy

Molčanová Zuzana<sup>1,a\*</sup>, Ballóková Beáta<sup>1</sup>, Miženkova Wanda<sup>1,2</sup>,  
Džupon Miroslav<sup>1</sup>, Zalka Dóra<sup>1,3</sup> and Saksl Karel<sup>1,3</sup>

<sup>1</sup>Institute of Materials Research, SAS, Watsonova 47, Košice, Slovakia

<sup>2</sup>Faculty of Mechanical Engineering, Technical University of Košice, Košice, Slovakia

<sup>3</sup>Faculty of Science, Pavol Jozef Šafárik University in Košice, Slovakia

<sup>a\*</sup>molcanova@saske.sk

**Keywords:** biodegradable alloys; magnesium based alloys; rapid solidification.

### Abstract.

From the point of view of possible medical applications, biodegradable alloys belong to the hot topic material. Many different systems are studied in this field, seeking a compromise between mechanical-physical properties vs. biocompatibility. Due to the suitable degradation rate, magnesium alloys, as well as zinc and iron, have been extensively investigated in recent years. The Mg<sub>66</sub>Zn<sub>30</sub>Ca<sub>4</sub> system is well known due to its promising mechanical properties and good biocompatibility. In this work, we want to present the way how to improve the mechanical properties of this alloy by yttrium substitution. The Mg<sub>66-x</sub>Zn<sub>30</sub>Ca<sub>4</sub>Y<sub>x</sub> (x = 0, 2, 4, 6) ingots were prepared by a rapid solidification process. The mechanical properties of modified alloys were compared with the starting alloy. The addition of Y (up to 4 at. %) leads to the improvement of ultimate compressive strength (Fig. 1, left). By Tafel plots (Fig. 1, right) the prediction of corrosion rates of analyzed samples was estimated. The higher amount of Y (above 4 at. %) causes decreasing in corrosion. The values of selected physical properties of the prepared alloys are listed in Tab. 1.

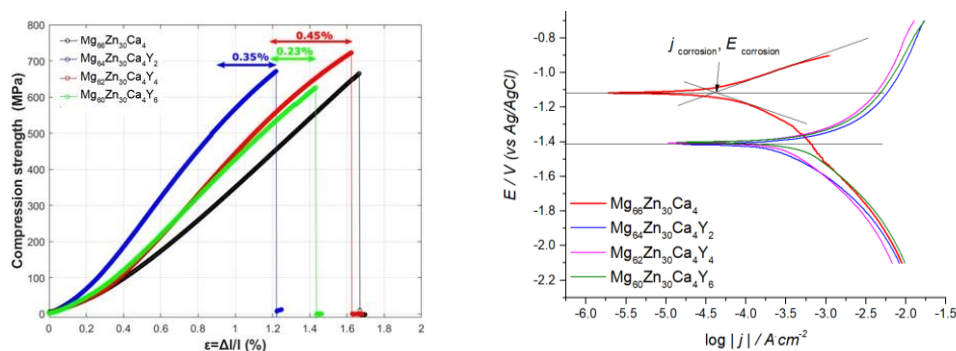


Fig. 1 The ultimate compressive strength of Mg<sub>66-x</sub>Zn<sub>30</sub>Ca<sub>4</sub>Y<sub>x</sub> (x = 0, 2, 4, 6) ingots (left). Tafel plots measured in Hank solution (pH = 7) at 33 °C.

Table 1 Mg<sub>66-x</sub>Zn<sub>30</sub>Ca<sub>4</sub>Y<sub>x</sub> (x = 0, 2, 4, 6) alloys density, compressive strength, Young modulus and corrosion rate data

Alloy	Density [g*cm <sup>-3</sup> ]	Ultimative Compressive Strength [MPa]	E [GPa]	Corrosion Rate (mm/y)
Mg <sub>66</sub> Zn <sub>30</sub> Ca <sub>4</sub>	2,967	662	46	0,8788
Mg <sub>64</sub> Zn <sub>30</sub> Ca <sub>4</sub> Y <sub>2</sub>	3,02	671	69	16,70338
Mg <sub>62</sub> Zn <sub>30</sub> Ca <sub>4</sub> Y <sub>4</sub>	3,065	723	58	18,49722
Mg <sub>60</sub> Zn <sub>30</sub> Ca <sub>4</sub> Y <sub>6</sub>	3,066	626	52	14,89093

### Acknowledgment

The authors are grateful to the Slovak Research and Development Agency under the contract No. APVV-17-0008 and APVV-20-0068.

## Evaluation of Sample Preparation Importance for Digital Image Correlation During Cold Deformation

Brić Tin<sup>1,a\*</sup>, Jandrić Ivan<sup>1,b</sup> and Mrkobrada Lorena<sup>1,c</sup>

<sup>1</sup>Faculty of Metallurgy, University of Zagreb, Aleja narodnih heroja 3, 44000 Sisak, Croatia

<sup>a\*</sup>tbrlic@simet.unizg.hr, <sup>b</sup>ijandri@simet.unizg.hr, <sup>c</sup>lrmkob@simet.unizg.hr

**Keywords:** digital image correlation (DIC); strain; sample preparation; cold deformation.

### Abstract.

The importance of the sample preparation in determining the displacements and strain amounts is one of the main challenges in the testing of metallic materials during cold deformation by digital image correlation (DIC).

In this paper, tests were performed by monitoring changes of strain amounts and their distribution by digital image correlation during static tensile testing of steel in accordance with standard DIN EN ISO 6892-1 B. The influence of different combination of speckles application on the sample surface (white speckles on the black sample surface and black speckles on the white sample surface) during cold deformation of steel was tested with the non-contacting digital image correlation. Strain amounts obtained by digital image correlation analysis of tested samples, with white-on-black and black-on-white painted speckle patterns, were compared, Fig. 1.

Different analysis for determining and monitoring strain amounts, provided by digital image correlation software, were used in this paper. The strain amounts were compared during cold deformation until the occurrence of sample fracture in both combinations of speckles application on the sample surface.

Research has shown the importance of proper sample preparation for determination strain amounts during cold deformation of tested steel.

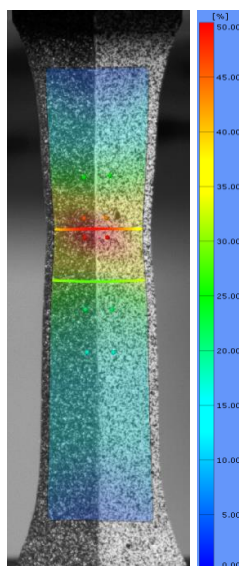


Fig. 1 Comparison of strain amounts in the region of white speckles on the black sample surface and black speckles on the white sample surface.

### Acknowledgment

This paper was supported by infrastructural scientific project VIRTULAB—Integrated Laboratory for Primary and Secondary Raw Materials, Code: KK.01.1.1.02.0022 funded by the European Regional Development Fund, Operational Programme Competitiveness and Cohesion 2014–2020.

## Creep Resistance and Microstructure Evolution in HR3C–P92 Heterogeneous Welds

Vodárek Vlastimil<sup>1,a\*</sup>, Kuboň Zdeněk<sup>2,b</sup>, Váňová Petra<sup>1,c</sup>,  
Palupčíková Renáta<sup>1,d</sup> and Langer Svatopluk<sup>1,e</sup>

<sup>1</sup>VŠB – Technical University of Ostrava, Faculty of Materials Science and Technology,  
17. listopadu 15, Ostrava – Poruba, Czech Republic

<sup>2</sup>MATERIAL AND METALLURGICAL RESEARCH, Ltd., Pohraniční 31, Ostrava –Vítkovice,  
Czech Republic

<sup>a\*</sup>vlastimil.vodarek@vsb.cz, <sup>b</sup>creep.lab@mmvyzkum.cz, <sup>c</sup>petra.vanova@vsb.cz,  
<sup>d</sup>renata.palupcikova@vsb.cz, <sup>e</sup>svatopluk.langer.st@vsb.cz

**Keywords:** heterogeneous welds; stress rupture tests; heat affected zone; microstructure evolution; minor phases.

### Abstract.

The paper deals with results of long-term stress rupture tests on „cross-weld“ specimens made of HR3C–P92 heterogeneous welds. Blunt circumferential welds of tubes  $\phi$  43 x 6 mm were manufactured by orbital TIG welding technology, using a filler material Thermanit 617. Preheating at 180 °C and interpass temperature up to 300 °C were applied during welding. After welding the weld joint was cooled down to 80-100 °C and immediately post weld heat treated at 760 °C, which is the regime typical for tempering of P92 steel.

Based on the results of stress rupture tests at 625 and 650 °C up to 20 000 hours to rupture, creep behaviour of heterogeneous welds was evaluated by comparison with a creep master curve for P92 steel which has a lower creep resistance than HR3C steel. Creep rupture strength values of HR3C–P92 welds for 10<sup>4</sup> hours at both 625 and 650 °C were calculated using the Larson–Miller parametric equation of the 1<sup>st</sup> order. Metallographic studies revealed that the preferential location of failure was the inter-critical part of the heat affected zone in P92 steel. Local changes of hardness during creep exposure were evaluated by microhardness profiles across the welds.

Microstructural characterization of individual parts of heterogeneous welds was carried out using light microscopy, scanning electron microscopy and transmission electron microscopy. Investigations were carried out on specimens in the as-received state and after the longest rupture times achieved during creep at 625 and 650 °C, respectively. A special attention was paid to precipitation reactions in individual parts of heat affected zones of both base materials.

Microstructure of the HR3C steel after quality heat treatment was formed by austenite and undissolved particles of Z-phase. Long-term exposure at 625 and 650 °C was accompanied by intensive precipitation of  $\sigma$ -phase, M<sub>23</sub>C<sub>6</sub> and secondary Z-phase. Particles of  $\sigma$ -phase formed networks along grain boundaries, fine secondary Z-phase particles preferentially nucleated on dislocations.

Microstructure of P92 steel after normalizing and tempering consisted of tempered martensite and particles of M<sub>23</sub>C<sub>6</sub> and MX minor phases. Chemical composition of MX phase corresponded to (V,Nb)N. Long-term exposure at 625 and 650 °C was accompanied by intensive precipitation of Laves phase which exhibited a high growth rate.

### Acknowledgment

This contribution was created with a financial support from the TACR project No. TK03020055 “Research of creep behaviour and verification of brittle fracture properties of austenitic steels for thermal power plant blocks with USC steam parameters” and the project No. SP2022/33 “Study of the relationship between the microstructure and properties of progressive technical materials, degradation mechanisms and behaviour of progressive technical materials in different operating conditions”.



# **EXHIBITOR PRESENTATIONS**

## From Data to Information With Selective BSE Contrast Methods of TESCAN's CLARA Field-Free UHR-SEM

Moravčik Igor

TESCAN ORSAY HOLDING, a.s., Libušina třída 21, 623 00 Brno, Czech Republic

igor.moravcik@tescan.com

**Keywords:** selective BSA contrast methods; TESCAN's CLARA Field-Free UHR-SEM.

### Abstract.

With the ongoing consolidation of UHR-SEM resolution performance, the evaluation criteria for UHR-SEM capabilities is slowly but surely placing more emphasis on the ability to use a wide diversity of contrast methods to reveal information that is not visible with resolution alone.

In general, when energy is transferred to the specimen by the primary beam, the sample generates a range of useful signals that are exploited to characterize the material. One of the principal signals generated by the sample, the backscattered electron signal (BSE), originates from all different depths below the surface of the sample at a range of angles and emitted energies. BSEs captured at different angles from the sample surface contribute differently to the imaging of sample morphology and potentially to grain orientation (channeling contrast). Low-energy loss BSEs reveal more surface detail than do high-energy loss BSEs. Thus, angular and energy-selectivity of the BSE signal are considered secondary backscattered electron contrast methods. It is evident that having the ability to acquire the BSE signal selectively can potentially enhance the information that a backscattered electron image reveals.

TESCAN CLARA UHR-SEM is tackling this requirement by implementing a comprehensive choice of backscattered electron detectors, including chamber-mounted segmented solid-state or scintillator backscattered electron detectors, an on-axis in-column detector, and the proprietary in-column Multidetector™. The Multidetector™ offers users the unique ability to discern signals by the energy of incoming BSEs and collect BSE contrast from the very surface of the sample.

The Multidetector™ is included in any TESCAN CLARA UHR-SEM base unit, which makes TESCAN CLARA a desirable tool for the curious Material Scientists that wish to explore their samples with the widest possible range of contrast methods to yield that piece of critical information that they seek.



**Tinius Olsen:** nabízí kompletní řadu stolních tvrdoměrů a mikrotvrdoměrů, samostatně stojících tvrdoměru a speciálních tvrdoměrů, které mohou být integrovány přímo do výrobní linky. Dodává kompletní sadu indentorů a referenčních bloků pro všechny stupnice tvrdosti.



**Thermo Scientific:** stolní rastrovací elektronové mikroskopy řady **Phenom** poskytují revolučně intuitivní způsob ovládaní, rychlou práci a kvalitní snímky jak z SED a BSD tak prvkové složení z EDS detektorů. Důraz je dále kladen na SW automatizaci snímání a vyhodnocení dat pro průmyslové použití.

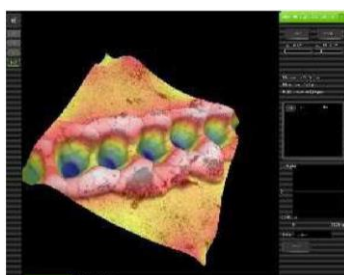
Authorized Distributor

### Phenom XL - ideální do průmyslu

- Velikost vzorku až 10x10x6,5 cm
- První elektronový snímek do minuty
- Rozlišení < 14 nm, zvětšení až 100 000x
- Motorizovaný stůl
- Optický a elektronový náhled pro rychlou orientaci a přesun kliknutím do oblasti zájmu
- Automatizace pomocí skriptování
- Jednoduchá obsluha, přívětivá cena



Držáky pro testování materiálů v tahu/tlaku v přístroji do 0,15 a 1 kN



3D rekonstrukce hrubosti povrchu



Eu- a kompu-centrický držák pro naklápění a rotaci se zachováním ostrého obrazu původní oblasti



Bližší informace o produktech těchto firem vám sdělíme na našem stánku, či je naleznete na webu [www.anamet.cz](http://www.anamet.cz)



ISBN: 978-80-553-4064-7

ABSTRACT BOOKLET  
Abstracts of Contributions from the  
18<sup>th</sup> International Symposium on Metallography,  
Fractography and Materials Science  
METALLOGRAPHY & FRACTOGRAPHY 2022